EVLA Memo 195
Jansky Very Large Array Primary Beam Characteristics

Rick Perley

June 8, 2016

Abstract

Results from recent measurements of the Jansky VLA's primary beams are presented. The total intensity beam profiles (Stokes 'I') are fitted with 3rd or 4th order polynomials. The coefficients are determined for all of the standard spectral windows for P through Ku bands. For the three highest frequency bands (K, Ka, Q), the coefficients for selected spectral windows are determined. The Stokes 'I' primary beam shapes are sufficiently similar across each of the high frequency bands from X through Q that a single set of coefficients (normalized for frequency) should be sufficient for most observations. The low frequency bands 'L', 'S', and 'C' have primary beams which are strong functions of frequency (beyond the normal frequency dependence) so that frequency-dependent coefficients must be utilized. The 'P' band primary beam is unique in that the defocussed feed creates a broad plateau underlying the central beam. A secondary benefit of this study is that I can confirm that all eight Cassegrain bands utilize the same definition of Stokes 'V'. All data products from this study have been archived for public access.

1 Introduction

Wide-field observations taken with radio telescopes suffer direction-dependent beam attenuation. As each of the four cross-correlations suffers a different (complex) modulation, correction requires careful measurements of the primary beam patterns in all four correlations. Measurements of the VLA's primary beam patterns were last done in 2000. Since that time, the EVLA Project has replaced the old narrow-band L, C, X, and Ku band horns with new wide-band ones, and new bands (S and Ka) have been added. The old beam attenuation functions measured in 2000 can not be expected to correctly describe the new systems. In addition, since the beam patterns are expected to vary as a function of frequency (beyond the wavelength scaling), they need to be measured across the entire bandwidth. This memo describes the basic results of new measurements, taken over the past 18 months, of the Jansky VLA's primary beams.

Correction for beam attenuation now takes two forms. The elementary method is to simply divide the output image by the antenna beam power pattern attenuation function. For this, it is convenient to have a highly oversampled measurement of the Stokes 'I' beamshape, out to, or perhaps a little beyond, the first null. This method is sufficient for most users, provided they are interested only in Stokes 'I', and the beams are close to circular, since knowledge of the parallactic angles of the observations is not needed.

For polarimetric observations, or for observations with antenna beams that are not circularly symmetric, a considerably more sophisticated (and time-intensive) approach is required, since in these cases, the correction function is not azimuthally symmetric and rotates about the field center as the observation progresses. For this method – known as 'A-Projection' – the need is to measure the (complex) aperture illumination functions in the relevent correlations (RR, RL, LR, or LL) with enough spatial resolution that the observed visibility function can be modified. This requires measurements of the primary beam out to at least the 4th null – but only modest oversampling is required.

2 The Observations

The observations were made using the holography observing mode. The code has been extensively modified (primarily by Michiel Brentjens) to permit properly rectangular observations for all offset angles – this is important for low frequency beam measurements where the curvature inherent in an alt-az mount severely distorts the sampling grid for large-angle offsets, particularly for observations taken at high elevations. For these observations,

each raster point was observed for 10 seconds, except at P-band, where the larger grid spacing required a longer integration time of 15 seconds.

All observations, except at P-band, were made with a square (l,m) grid, where the coordinates are the offset direction sines defined w.r.t. the beam center, 'l' points to the right (looking outwards), and 'm' points to the local zenith. The sampling motion alternates direction for each row or column. Normally the most rapid motion is taken in the 'l' coordinate (mostly azimuth), but at low frequencies, due to the large azimuth motions required for large offsets at high elevations, the primary motion is often chosen in the vertical direction.

At P-band, because of the length of the observation and the high elevation of the target source 3C147 near transit, the observations were broken into two segments. The intention was to measure separately the lower and upper halves of the beam pattern, each with a 41x21 grid, at early and late hour angles. However, due to a blunder, the offsets were twice what was intended, resulting in a 41 x 21 rectangular gap in the center – the region spanning the main beam. Hence, a third obervation to cover the gap was required, resulting in a total 41 x 61 grid, spanning a considerably larger angle in the vertical direction than was intended.

A short amplitude and phase calibration scan was performed at the end of each row or column. Although the phase is not important for the beam total intensity profiles, the full complex response is needed for the 'W-Projection' algorithm (and for all polarimetry).

All observations were taken with full polarimetry in mind. This requires sufficient parallactic angle coverage to derive a good solution of the on-axis instrumental cross-polarization, plus an observation of a source of high linear polarization with a known position angle. For this, the sources 3C286 or 3C138 were used. In addition, pointed observations of the target source at eight offsets at the half-power in the N, S, E, W, NW, SW, NE, and SE directions were made, as a check of the holography offset positions.

Source polarization is a complication to the beam parameter measurements which is most easily avoided by choosing a target object known to be unpolarized. The target source must also be strong, as we need good SNR in the sidelobes, and preferably unresolved[1]. It is generally important to avoid observations at high elevations, as the large offsets required at the lower frequencies require very large azimuth motions at high elevations. Furthermore, accurate beam tracking for our alt-az telescopes is considerably degraded at high elevation – this is especially important at high frequencies. These conditions impose severe constraints on the choice of target source. I have used 3C147 for observations at P through Ku bands, J0609-1542 for Ku and Ka bands, and 3C84 (J0319+4130) for Q band. To minimize pointing errors, referenced pointing was utilized at all bands except P. For L through K bands, this was done once per hour. For Ka and Q bands, referenced pointing was done once every 20 minutes.

The observing regimen is to uniformly sample the beam pattern out to some sidelobe. The maximum angle is set by the offset of the Nth sidelobe at the lowest frequency in the band, while the sample increment (step size) is set by the oversampling factor at highest frequency in the band. This is easily quantified: For a uniformly illuminated circular aperture, the nulls in the power pattern occur at approximately $\theta \sim 1.25\lambda/D$. Hence, if we wish to sample out to the N^{th} sidelobe at the lowest frequency, the maximum offset angle is:

$$\theta_{max} \sim \frac{1.25 N \lambda_{max}}{D}. \tag{1}$$

The stepsize is set by the oversampling necessary at the highest frequency. If we want to oversample by factor M at the highest frequency, the stepsize must be

$$\theta_{min} \sim \frac{\lambda_{min}}{MD}. \tag{2}$$

Hence the length of a raster line, N_{pts} is

$$N_{pts} = 1 + 2\frac{\theta_{max}}{\theta_{min}} = 1 + 2.5N \cdot M \cdot BWR \tag{3}$$

where $BWR = \nu_{max}/\nu_{min}$ is commonly called the bandwidth ratio. For high bandwidth ratios, large angles and dense sampling, the raster size can be very large: With $N = 4$, $M = 3$ and $BWR = 2$, the grid size is 61 x 61, requiring over 10 hours, not counting calibration time.

For the lowest three bands (P, L, and S), highly oversampled observations were made out to the third or fourth null. This is a time-intensive process (eleven hours was required to sample the S-band beam out to the 4th null at the low frequency end, with 4 times oversampling at the high frequency end), which required a different approach for the higher frequency bands.

[1]The condition is less stringent than may be imagined. Since the holographic data are baseline-based, it is only required that the target source extent be $\leq$10% of the beamwidth.

Thus, for the remaining bands, a two-pronged approach was taken. For the simple beam correction method, the primary beam was sampled out to the first null at the low-frequency end of the band, with 4X oversampling at the high frequency end. For the aperture plane ('A-Projection') method, the beam pattern was sampled to the 4th null at the low frequency end, with 1.5X oversampling at the high frequency end. This reduced the time needed to typically 2.5 hours.

The 8-bit sampling mode was selected for all observations, primarily because of concerns about the stability and linearity of the 3-bit mode. Most importantly, the possible need to utilize the switched power gain monitoring system drove this decision[2]. This requires more frequency tunings, since the 8-bit system spans only 2 GHz while the 3-bit mode spans 8 GHz. Ideally, we want to cover the entire 1 – 50 GHz range of the VLA, but this was not practical given the time constaints and the use of the 8-bit system. Thus, the three highest frequency bands do not have full frequency coverage, but have been sampled with four frequency 'chunks', each 1.024 GHz wide.

Table 1 gives the parameters of all the observations.

Table 1: **Log of Beam Observations**

Band	Date dd/mm/yy	Dur. Hr	Time [a] hh:mm	Frequency GHz	Source	Δ [b] arcmin	Grid	MaxAng arcmin	Null [c]	Samp[d]
P[e]	23/07/15	8.7	all	.224 – .480	3C147	32.3	41x42	646x646	3.5x5.3	2.7
	24/09/15	4.3	all	.224 – .480	3C147	32.3	41x21	646x323	3.5x1.8	2.7
L	08/06/14	4.1	all	1.01 – 2.03	3C147	5.16	35x35	87.7	2.1	3.9
S	22/09/15	10.4	all	1.99 – 4.01	3C147	2.62	57x57	73.3	4.2	3.9
C	14/01/16	3.1	<05:20 [f]	3.99 – 6.01	3C147	1.72	17x17	13.7	1.3	4.0
			>05:20			4.59	23x23	50.5	4.9	1.5
	18/01/16	2.9	<05:10	5.99 – 8.01	3C147	1.28	17x17	10.2	1.5	4.0
			>05:10			3.40	21x21	34.0	4.9	1.5
X	16/01/16	2.6	<05:05	7.99 –10.01	3C147	1.03	15x15	7.21	1.4	4.0
			>05:05			2.75	21x21	27.5	5.3	1.5
	17/01/16	2.3	<05:10	9.99 –12.01	3C147	0.86	15x15	6.02	1.5	4.0
			>05:10			2.28	19x19	20.5	5.0	1.5
Ku	19/01/16	2.5	<05:06	12.0 – 14.0	3C147	0.74	15x15	5.15	1.5	4.0
			>05:06			1.96	19x19	17.6	5.1	1.5
	20/01/16	2.3	<05:08	14.0 – 16.0	3C147	0.64	15x15	4.51	1.5	4.0
			>05:08			1.72	19x19	15.5	5.3	1.5
	22/01/16	2.3	<05:12	16.0 – 18.0	3C147	0.57	15x15	4.01	1.6	4.0
			>05:12			1.53	19x19	13.8	1.5	1.5
K	23/01/16	2.3	<04:45	19–20,21–22	J0609	0.47	15x15	3.27	1.5	4.0
			>04:45			1.25	19x19	11.2	5.2	1.5
	24/01/16	2.3	<05:02	23–24,25–26	J0609	0.39	15x15	2.61	1.5	4.0
			>05:02			1.05	19x19	9.45	5.3	1.5
Ka	29/01/16	2.6	<04;13	28–29,34–35	J0609	0.29	15x15	2.04	1.4	4.0
			>04:13			0.78	19x19	6.99	4.7	1.5
	07/02/16	2.6	<03:22	31–32,37–38	J0609	0.27	15x15	1.87	1.4	4.1
			>03:22			0.71	19x19	6.40	4.8	1.5
Q	09/02/16	5.7	<03:33 [g]	41–42;43–44	3C84	0.22	15x15	1.56	1.6	4.2
			>04:34			0.59	19x19	5.33	5.3	1.6
			<04:34	46–47;48–49	3C84	0.20	15x15	1.40	1.6	4.2
			>06:06			0.53	19x19	4.79	5.3	1.6

[a]The IAT time for the grid

[b]The grid spacing in arcminutes

[c]The offset null number at the lowest frequency for uniform illumination

[d]The oversampling factor at the highest frequency

[e]Three separate observations were combined, providing a grid 41x61

[f]< means times up to this time, > means: times after this time

[g]The low frequency, oversampled data were taken before 3:33IAT, the high frequency, oversampled data between 3:33 and 4:34, the low frequency, sparsely sampled grid between 4:34 and 6:06, and the high frequency, sparsely sampled grid after 6:06 IAT

The observations in P, L, and S bands were done in the A configuration to minimize the possibility of cross-

[2]Self-calibration can not be used in holography to remove gain variations!

talk between the antennas. All other observations were made in C configuration, as at these bands good phase stability is important[3], while cross-talk is a negligible issue at high frequencies. For the highest frequency bands, observations must be made in calm weather and clear skies, as both pointing accuracy and phase and amplitude stability are critical.

To protect against possible atmospheric phase instability, multiple reference antennas were employed in all observations. Typically, seven reference antennas were employed, one at the center, one at or near the end of each arm, and one about halfway down each arm. This prevents measurement of the beam patterns for those antennas, but since the primary goals were to determine the median beam response, and the spread in response, measurement of each individual antenna's pattern is not (yet) required.

The correlator setup was the normal 'continuum' mode with full polarization, providing maximum bandwidth coverage with 16 spectral windows, each with 64 spectral channels, for each frequency tuning. The spectral window width is 16 MHz at P-band, 64 MHz at L-band, and 128 MHz at all other bands. With two simultaneous frequency tunings available, the bandwidth coverage was 256 MHz at P-band, 1024 MHz at L-band, and 2048 MHz at all other bands. The integration/dump time was 1.0 seconds – which permits efficient removal of the data taken while the antennas were moving from one point to the next – this typically took 3 – 5 seconds.

3 Analysis

Basic calibration was done in AIPS, following standard procedures, so no specific description is given here. In general, phase and amplitude stability were very good for all observations. All data were Hanning smoothed to protect against spectral ringing. The behavior of the antennas is of course never perfect, so careful editing of all data was required to ensure only well-behaved antennas were utilized in the beam measurements. Issues particular to each observation are given in the discussions below. Visible RFI was either flagged by removing specific channels known to be continuously affected (via UVFLG), or by using CLIP to remove amplitudes above a nominated value, typically set to about 7σ. This simple approach is especially effective when the cross-hand flags are applied to the parallel-hand visibilities.

Following the editing and calibration steps, the data were broken into individual spectral windows using 'UVCOP'. This step was taken only to speed up extraction of the data for subsequent analysis. However, the task 'UVCOP' rescales the (u,v) values to the new reference frequency of the output database. This is appropriate for normal (u,v) data, but is not wanted in holography, as (at least in AIPS) the (u,v) coordinates values are replaced with (l,m) beam offset angles – which are the same for all spectral windows, and hence do not need rescaling. The effect of the rescaling is to expand the measured beams for all but the lowest frequency spectral window! This undesirable effect is taken out in the next step, as related below. Note that this problem is avoided if the original multi-spectral window database is used for the data extraction – but at the cost of greatly increasing the (wall-clock) execution time.

As the data were taken in holography mode, the AIPS holography program UVHOL is advised for extraction of the holography data. This program 'understands' the VLA's holography modes, and allows a wide range of useful operations, including

- The adverb WTUV undoes the scaling error introduced by the action of UVCOP described above. This parameter is set to (old reference frequency)/(new reference frequency). Normally, this would be the ratio of the central frequency of the first spectral window to the central frequency of the extracted central frequency.
- The adverb ANTENNAS identifies the reference antennas requested for the output. When APARM(5)=1, the data are averaged over all named reference antennas.
- The adverb BASELINES identifies the target (moving) antennas. When APARM(8)=1, the data are averaged over all named target antennas.
- The adverb NPOINTS identifies the number of good samples to be retained at each pointing position. This allows data taken while the antennas are moving from one position to the next to be discarded. When APARM(6)=1, all good samples within each pointing position are averaged together.
- The individual correlator outputs (RR, RL, LR, and LL), or the Stokes combinations (I, Q, U, V), or subsets therof, can be extracted.

[3]For intensity only corrections, the phase stability need only be stable within the 10-second dwell on any one point. However, for full polarization, corrections require accurate phase, so good phase stability spanning the calibration timescale is required.

The output from UVHOL can be written to the terminal screen (OPCOD = ") for review, or to a disk file specified by the 'OUTPRINT' adverb. The output file contains important header information (identified by '#!' at the beginning of each line), followed by the data in columnar format. The columns give the measurement angles $\sin l$ and $\sin m$, the amplitude and phase (or real and imaginary parts), and estimated errors of the amplitude and phase (or real and imaginary parts). The header data include the reference antenna(s), target antenna(s), correlation product or Stokes combination, frequency, the number of timestamps averaged, the spectral window number, the channel number, the time range from which the data are taken, the range of channels averaged to form the output, and whether the calibration and polarization calibration have been applied.

The files output by UVHOL are read by PBEAM, which fits polynomial coefficients to the two-dimensional sample grid. This program, originally written by Leonia Kogan, and extensively modified by Eric Greisen, fits the following radial function

$$P(r) = P_0 + P_2 r^2 + P_4 r^4 + P_6 r^6 + \cdots \quad (4)$$

where the radial variable 'r' is in normalized units: $r = R\nu_G$, where R is the offset in arcminutes and ν_G, is the frequency in GHz. The program also solves for the pointing center offsets. Optionally, the beam ellipticity and position angle are solved for. The program provides these parameters for a single input file, or can read two input files – the RR and LL grids – and from these determine the mean 'I' beam paramters, and the (squint) offset and orientation. The program provides error estimates, and displays the fits and residuals on screen to aid the user in finding the best fit. A more detailed description is given in the 'HELP' file.

Although fits with up to 9 terms are permitted, experience shows that third order (i.e., P_0 though P_6 is sufficient for an excellent description. We normally generate normalized polynomials ($P_0 = 1$), and utilize data to the 5% power level. Beyond this level the beams becomes inreasingly non-azimuthally symmetric, due to the influence of the support quadrupod.

To measure the change in beam pattern as a function of frequency within each band, each of the 16 spectral windows for each frequency tuning were analyzed separately. The coefficients for each are given in the tables in the following section.

All the calibrated data, in both FITAB and FITTP format, have been written to locations where any interested party can obtain them. Additionally, the extracted data (output from UVHOL) used for the results given in the memo have also been archived for subsequent analysis. The locations for these files are given later in the memo.

4 Results

Here I show the results from each band in a separate sub-section.

4.1 P-Band

The P-band feed is located approximately 70 cm below the effective prime focus, leading to a severely defocussed beam. The major effect is to eliminate the first null, and to replace the first diffraction sidelobe with a broad and relatively flat circular 'plateau'. The amplitude of the plateau rises from typically 2% of the peak of the beam at 235 MHz to more than 10% of the peak at 470 MHz, while the diameter declines from ∼18 degrees at the low end of the band to ∼9 degrees at the high end.

This situation is best illustrated in Figure 1, showing the voltage amplitudes in Stokes 'I' in 15 of the spectral windows. A linear transfer function has been used, saturating at about 70% of the peak.

One of the goals was to determine the spread in beam response amongst the pointing antennas. Figure 2 shows the Stokes 'I' profiles amongst the antennas, for 344 MHz. The spread is quite large – about 12% at the half-power.

Unlike the higher frequency bands, which are fed with wideband horns, the P-band feed is a simple crossed dipole. Unsurprisingly, there is also a wide variation in primary beamwidth and shape over the wide fractional bandwidth. This is illustrated in Fig 3, showing the average beam profiles for 14 of the spectral windows. Since the current feeds are unchanged from pre-EVLA times, little change is to be expected in the fitted beam profiles. That this is true is shown by the thick dashed line in the figure, which is the profile described by the current default polynomial, derived from data taken in 2000 at 327 MHz.

Fitting the beam with simple polynomials is not easy if the 'plateau' is to be accurately described. I settled for an expression accurate to ∼1% out to the 5% power level – this required four terms. The coefficients are shown in Table 2. The rms of the fit was fairly good – typically 1.5%. For these fits, all target antennas were

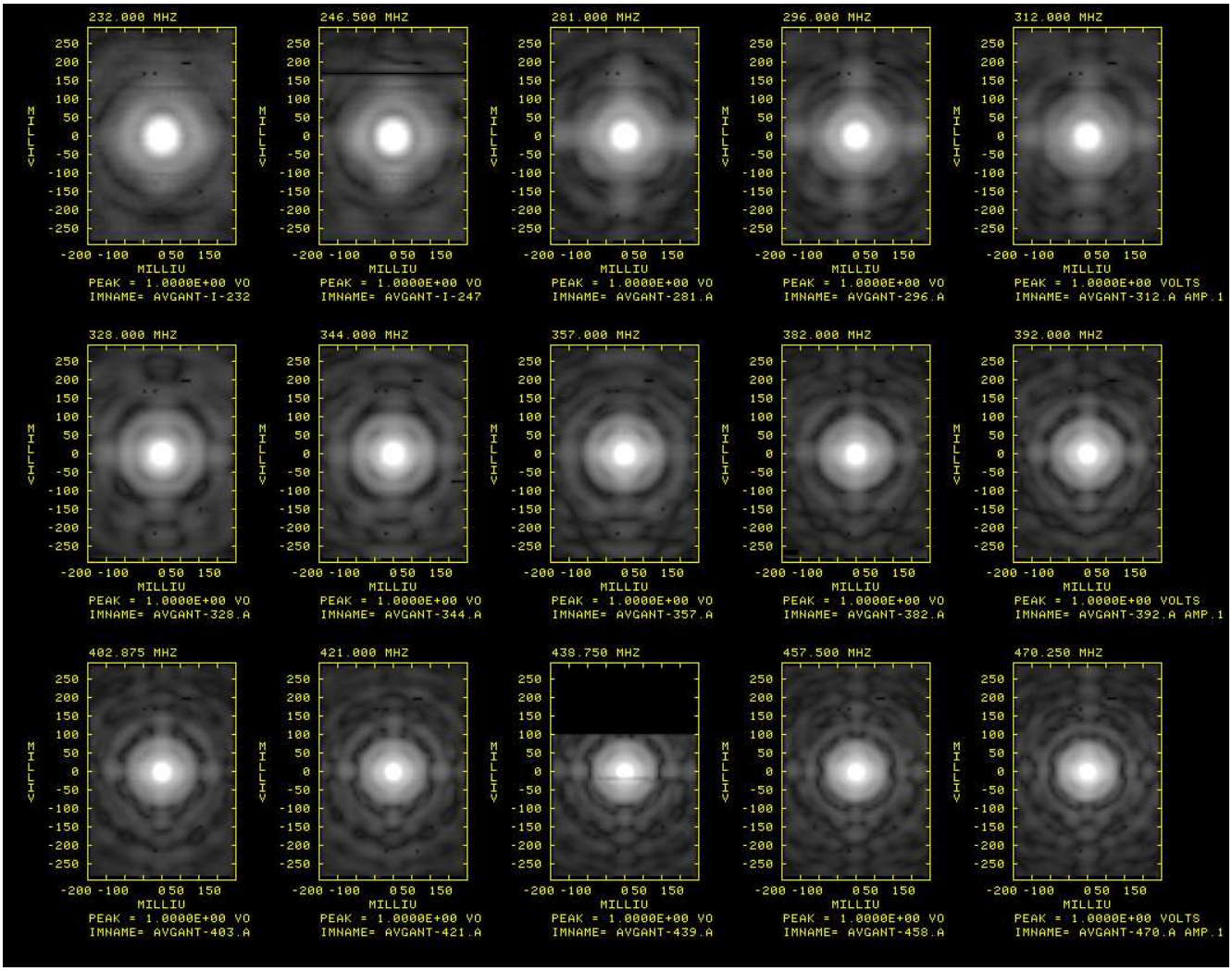

Figure 1: Grey-scale images of the P-band voltage primary beam, in 15 of the 16 spectral windows. The field of view is 21.6 by 32.7 degrees. The frequency increases from top left to lower right. The black region in the middle of the bottom row is due to exceptional interference on the first day of this three-day observation set. The effect of the mis-focussed feed is to nearly eliminate the first null, and to replace the first diffraction sidelobe with a broad, circular plateau, as shown by the circular disk surrounding the main beam.

summed against all reference antennas. The dofocussing plateau is easily visible in these fits, with the level rising steadily with increasing frequency.

Specific notes for these data:

- Reference antennas were 02, 04, 07, 08, 13, 15, 16, 17, 20, 24, 25
- SPW03 was obliterated by RFI for all three observation dates.
- SPW14 was ruined by RFI for the first of the three observations. The same RFI source created sufficient gain instability that no primary beam fits were possible in this window.
- ea22 was out on all three observations. ea05 was out on the first two observations. ea18 was out in the 'YY' polarization on all three dates. ea09 was out in the second observation. ea24 was bad in the 'XX' polarization on the third date.
- Hence, the antennas utilized for the fits were 01, 03, 06, 10, 11, 12, 14, 19, 21, 23, 26, 27, 28.

The wide variance in primary beam shape between antennas, and as a function of frequency will complicate accurate primary beam attenuation correction at this observing band.

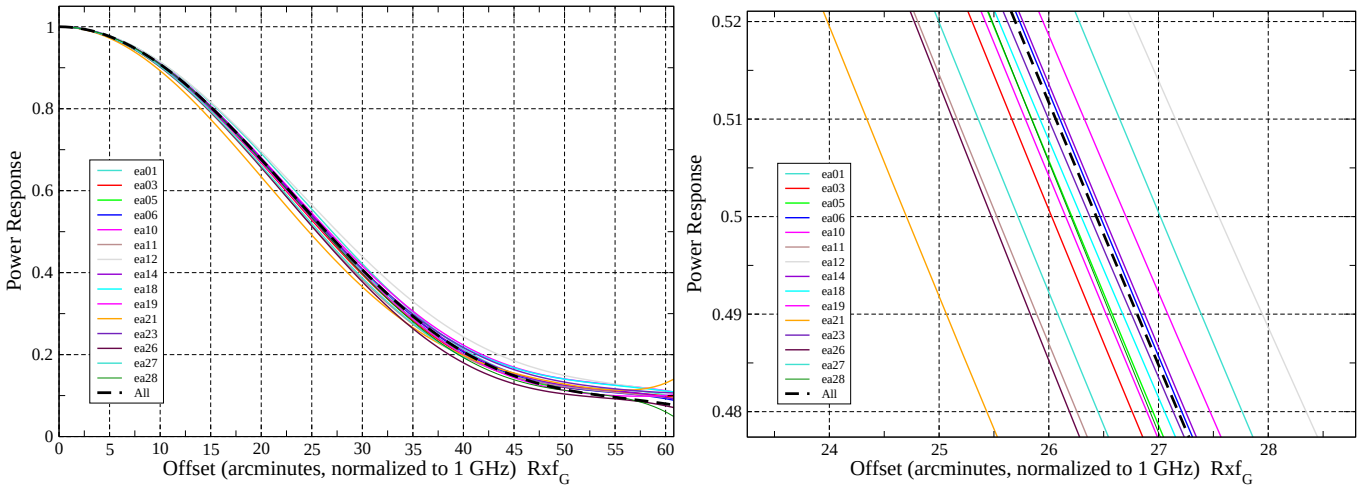

Figure 2: The primary beam shapes as a function of antenna at 344 MHz. The right panel is a zoom-in of the central region. There is a wide variation in beamwidths amongst the antennas – approximately 12%.

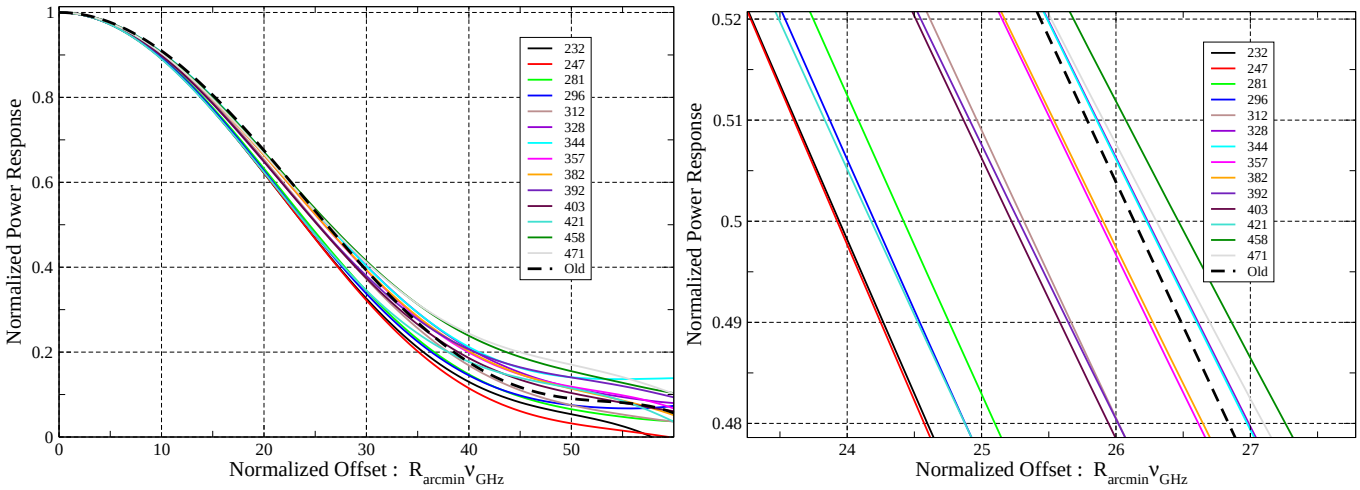

Figure 3: The primary beam shapes as a function of frequency across P-band. The right panel is a zoom-in of the central region. The dashed black line is the fitted shape at 327 MHz from observations in the 1990s.

4.1.1 Data Archive Locations

All three fully calibrated databases have been archived on the ftp server at:
/home/ftp/pub/staff/rperley/BeamHoloDat/PBand/PHOLO-n-FITxx
in both 'FITTP' and 'FITAB' formats, where 'n' is 1, 2, or 3 (corresponding to the first, second, or third observation), and 'xx' is either 'AB' or TP'. Note that the data from the central portion of the beam are in the third database. Each file is about 200 GB.

Additionally, the 'UVHOL' output files used for the analysis presented here have been stored on disk at
/users/rperley/BeamData/PBand/ALLP-SPWnnxx01
where 'nn' is the spectral window number (01 through 16, excepting 03), and 'xx' is one of 'I_', 'XX', or 'YY'. These data have the calibration applied, are averaged over the central 4 MHz of each spectral window, and are the average of all good moving antennas (1, 3, 6, 10, 11, 12, 14, 19, 21, 23, 26, 27 28) against all good reference antennas (2, 4, 7, 8, 13, 15, 16, 17, 20, 25).

Table 2: **Polynomial Fits for P-Band**

Freq. MHz	A_0	A_2 $\times 10^{-3}$	A_4 $\times 10^{-7}$	A_6 $\times 10^{-10}$	A_8 $\times 10^{-14}$	HWHM Arcmin.GHz
232	1.0	-1.137	5.19	-1.04	0.71	23.9
246	1.0	-1.130	5.04	-1.02	0.77	23.9
281	1.0	-1.106	5.11	-1.10	0.91	24.4
296	1.0	-1.125	5.27	-1.14	0.96	24.2
312	1.0	-1.030	4.44	-0.89	0.68	25.3
328	1.0	-0.980	4.25	-0.87	0.69	26.3
344	1.0	-0.974	4.09	-0.76	0.53	26.2
357	1.0	-0.996	4.23	-0.79	0.51	25.9
382	1.0	-1.002	4.39	-0.88	0.64	25.9
392	1.0	-1.067	5.13	-1.12	0.90	25.3
403	1.0	-1.057	4.90	-1.06	0.87	25.2
421	1.0	-1.154	5.85	-1.33	1.08	24.2
458	1.0	-0.993	4.67	-1.04	0.88	26.5
470	1.0	-1.010	4.85	-1.07	0.86	26.3

Typical fit rms is 1.5%. Typical errors in the five coefficients are .01, .028, .28, .11, and .13, in the units given. Coefficients based on all target antennas against all reference antennas.

4.2 L-Band

The raster is 35 x 35 points, with $\sim$ 4 x oversampling at the high frequency end, out to the 2nd null at the low frequency end. The data are of excellent stability and quality. A nice impression of the quality of data is shown in Fig. 4, showing fifteen Stokes 'I' beams in voltage, with a linear transfer function saturating at about the 50% voltage level. Prominent is the first diffraction sidelobe, at about 20% voltage (about 4% power). The axes are defined such that the beams are as seen on the sky, viewed from behind the antenna.

Third-order beam fits (to 5% power) were made for all operating target antennas at 1488 MHz to check on the distribution of the beam shapes amongst antennas. The results are shown in Fig 5. The spread in power between the antennas is about 3%, at the median 50% power level – corresponding to a similar fractional spread in FWHM. The mean beam shape parameters as a function of frequency were determined from the average of all moving against all reference antennas, using a third-order fit, for each of the 15 RFI-free spectral windows. For this the central 26 MHz of each spectral window was summed. The results are shown in Figure 6. The black dashed line shows the old beam profile at 1465 MHz, taken from 2000 data using the original feed. The new feed generates a beam about 3.5% smaller than the old feed at this frequency. The new coefficients are given in Table 3.

Table 3: **Polynomial Fit Parameters for L-Band**

Freq. MHz	A_0	A_2 $\times 10^{-3}$	A_4 $\times 10^{-7}$	A_6 $\times 10^{-10}$	HWHM	Freq. MHz	A_0	A_2 $\times 10^{-3}$	A_4 $\times 10^{-7}$	A_6 $\times 10^{-10}$	HWHM
1040	1.000	-1.529	8.69	-1.88	20.40	1552	1.000	-1.435	7.54	-1.49	20.03
1104	1.000	-1.486	8.15	-1.68	20.69	1616					
1168	1.000	-1.439	7.53	-1.45	20.98	1680	1.000	-1.443	7.74	-1.57	20.02
1232	1.000	-1.450	7.87	-1.63	20.99	1744	1.000	-1.462	8.02	-1.69	20.91
1296	1.000	-1.428	7.62	-1.54	21.15	1808	1.000	-1.488	8.38	-1.83	20.76
1360	1.000	-1.449	8.02	-1.74	21.06	1872	1.000	-1.486	8.26	-1.75	20.73
1424	1.000	-1.462	8.23	-1.83	21.00	1936	1.000	-1.459	7.93	-1.62	20.92
1488	1.000	-1.455	7.92	-1.63	20.95	2000	1.000	-1.508	8.31	-1.68	20.51

Typical rms of the fit: 0.5%. Typical errors in the parameters are .003, .020, .30, .10, in the units given. The units for HWHM are arcmin-GHz.

There is clear evidence that the normalized beam width is smaller at the lowest frequencies in this band – this is an expected result from the undersized feed, which over-illuminates the subreflector at the low frequency end. Discussion of this is deferred to a later section.

Specific notes for these data:

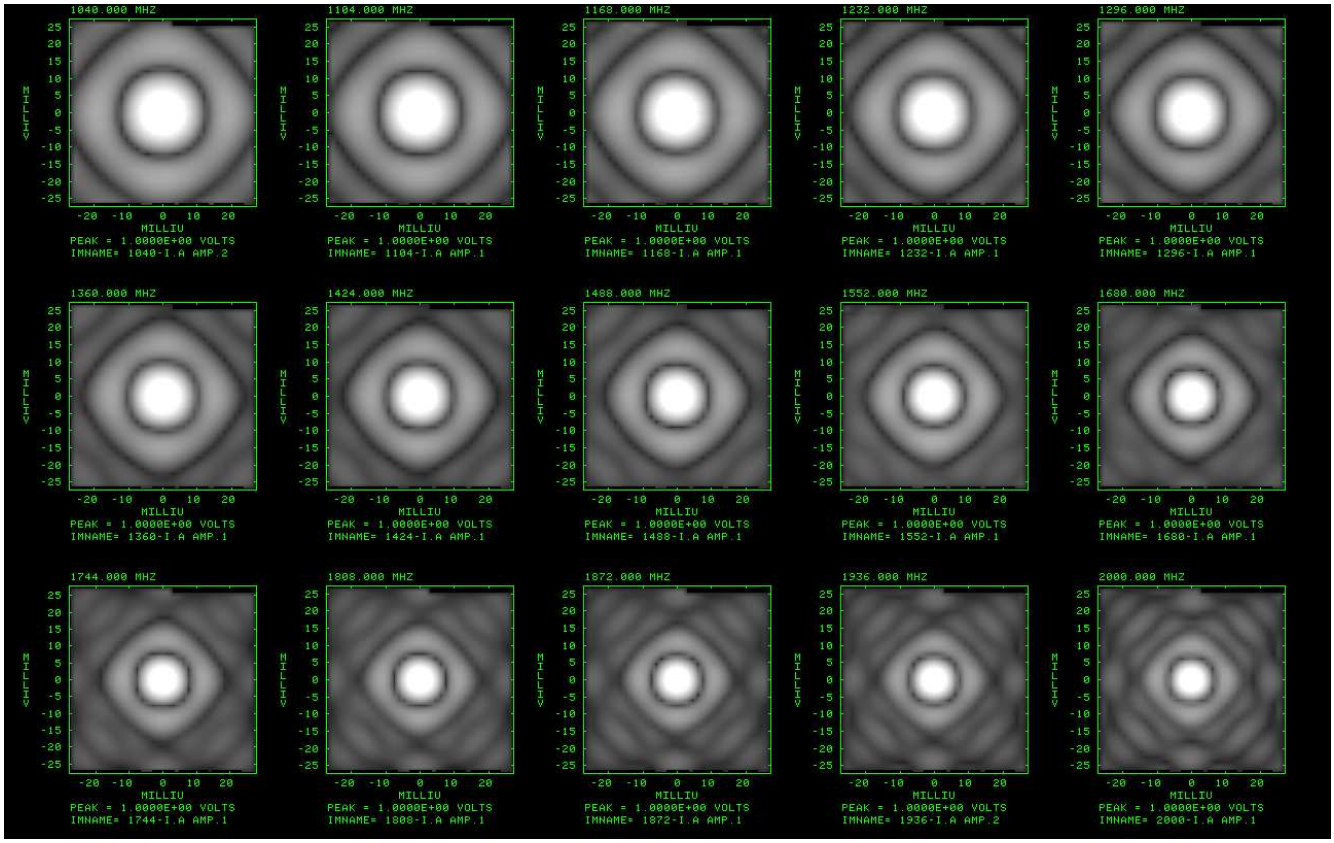

Figure 4: Grey-scale illustrations of the voltage primary beams at L-band for 15 of the 16 spectral windows. The field of view is 2.9 degrees. A linear greyscale is used, saturating at $\sim 50\%$ level.

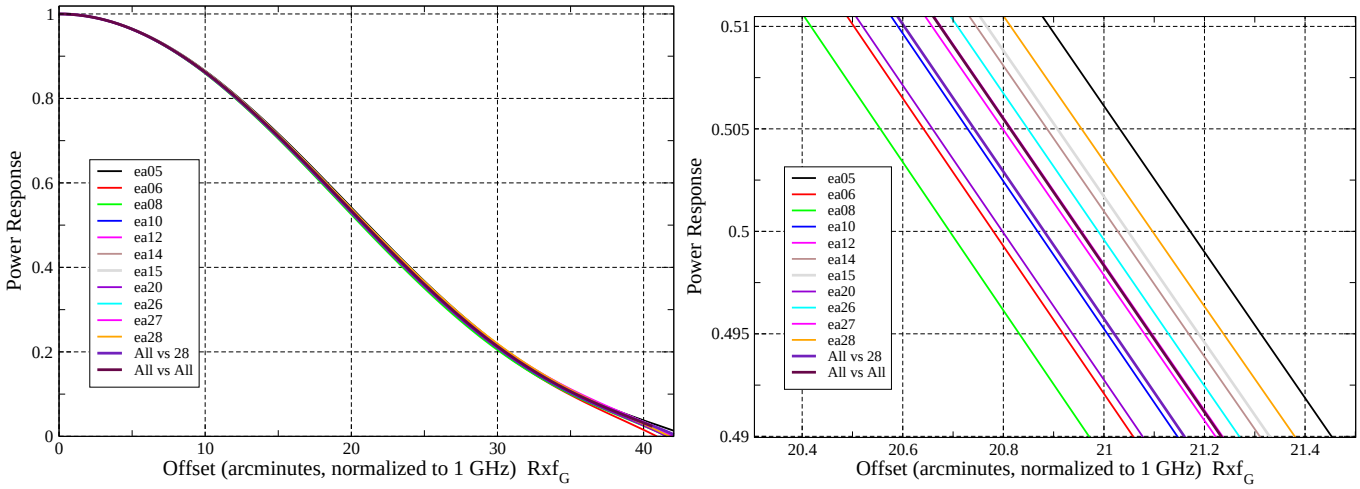

Figure 5: The variation in beam shape amongst 11 VLA antennas at 1488 MHz. The right panel is a zoom-in of the half-power region. There are no discrepant antennas amongst these. The power variation amongst the remaining antennas has a maximum $\sim$3% spread at the half-power point.

- Reference antennas were: 01, 02, 03, 04, 07, 09, 11, 17, 21, 22, 24, and 25.
- Antennas 16, 18 and 19 were out of the array
- Antenna 13 provided no LCP data for spectral windows 1 through 8
- Antenna 23 provided no useful data at all.

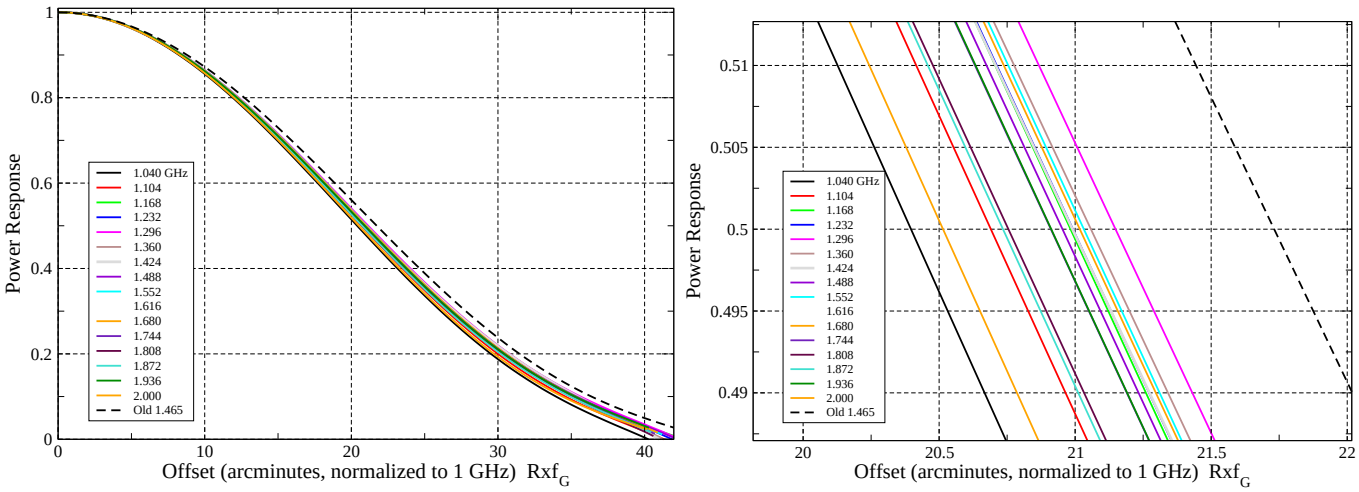

Figure 6: The primary beam shapes as a function of frequency across L-band. The right panel is a zoom-in of the central region, and clearly shows that the (normalized) half-width of the primary beam is less at the lowest three SPW than the others. The black dashed line is the fitted beam profile at 1465 MHz from 2000 observations, using the old VLA feed.

- Antenna 02 provided faulty data on the LCP side in spectral windows 2, 3, 6, and 7.

Affected data are flagged.

4.2.1 Data Archive Location

The calibrated database has been archived on the ftp server at:
/home/ftp/pub/staff/rperley/BeamHoloDat/LBand/LHOLO-FITxx
in both 'FITTP' and 'FITAB' formats, where 'xx' is either 'AB' or TP'. The files are about 180 GB. These two files include the calibration tables, to enable users to re-calibrate the data, if they so decide. Files with the calibration already applied are available at:
/home/ftp/pub/staff/rperley/BeamHoloDat/LBand/LHOLO-FITxx-CAL
in both 'FITTP' and 'FITAB' formats.

Additionally, the 'UVHOL' output files used for the analysis presented here have been stored on disk at
/users/rperley/BeamData/LBand/Lffffpp01
where 'ffff' is the central frequency in MHz of the spectral window (given in Table 3), and 'pp' is the Stokes polarization, one of: RR, RL, LR, LL, I_, Q_, U_, or V_. The data are fully calibrated, averaged over the central 17 MHz of each spectral window, and are the average of (target) antennas 5, 6, 8, 10, 12, 14, 15, 16, 20, 26 and 27 with the reference antennas 1, 3, 4, 7, 9, 11, 17 21 22 24 and 25.

4.3 S-Band

The beam observations at this band are the most complete of all – reflecting most likely its upcoming use for the VLASS. The basic observational parameters are given in Table 1. Within this band are the transmissions from two geostationary satellite systems, one of which (Sirius and XM satellite radio) has a significant effect on S-band performance. The third spectral window (spanning 2344-2372 MHz) has been removed from the analysis, due to severe interacation with the Sirius/XM transmission band. The second spectral window also sees a geostationary system, but here the disruptions are limited to a 20 MHz-wide block within the spectral window (2182 – 2202 MHz). The channels corresponding to these have been removed, and the remaining channels are fine. About halfway through the run, Sirius satellite S3 [4] passed within 20 degrees of 3C147, the target source. The increased signal strength caused a notable depression in the analog gains which was thus seen in all spectral windows. These were well corrected by application of the switched power gain monitor system.

Fifteen of the voltage primary beams are shown in Fig. 7. These are the beams as seen from behind, projected onto the sky. The grey-scale is linear, saturating near 50% voltage.

[4]The Sirius system is not geostationary, but employs a highly elliptical orbit with apogee over the central US, with a 24 hour period.

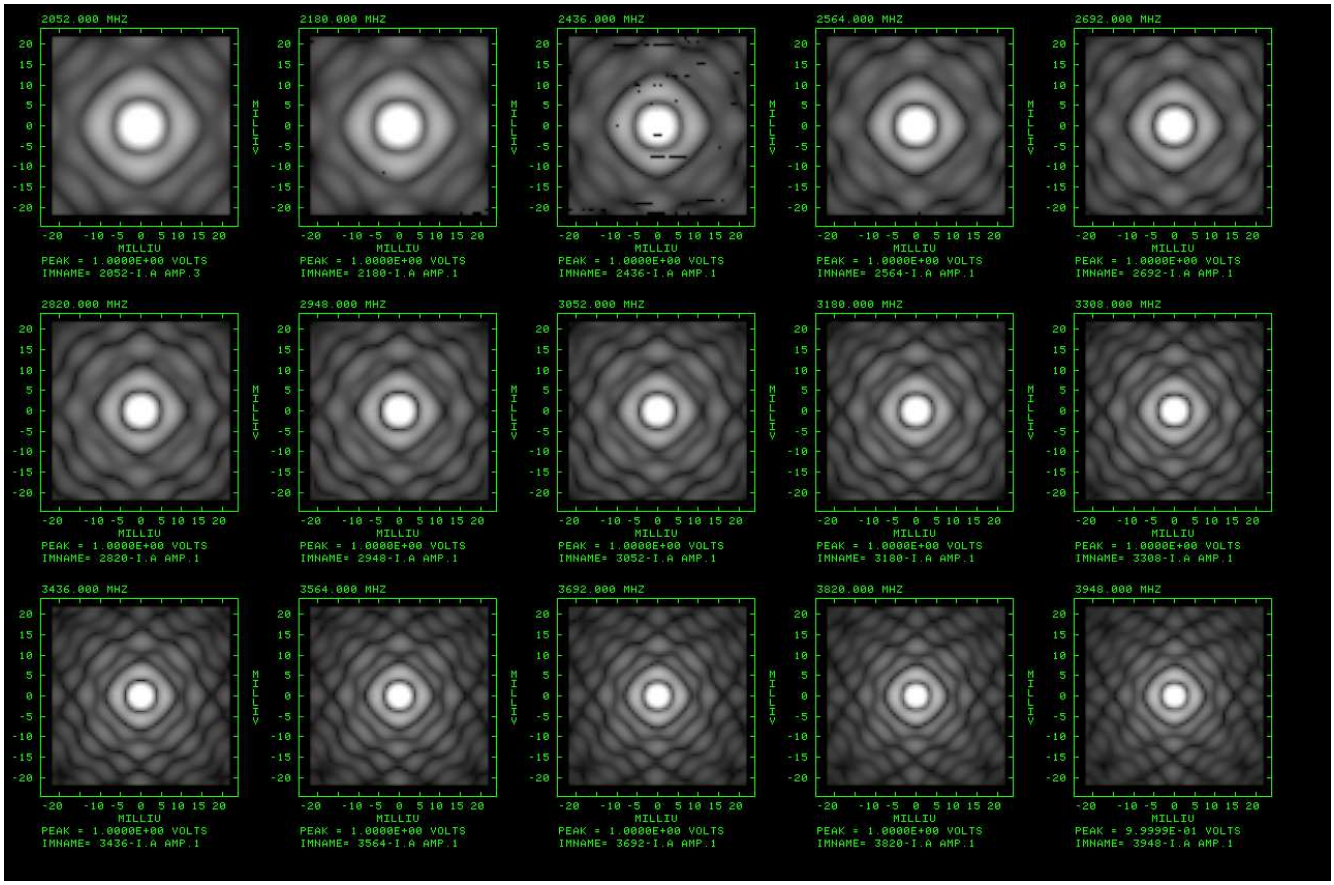

Figure 7: The S-band voltage beams for 15 of the 16 spectral windows. The field of view is 147 arcminutes. The greyscale is linear, saturating at about 50% voltage.

The 2948 MHz data for the good moving antennas (1, 2, 6, 8, 11, 12, 13, 14, 15, 16, 17, 19, 21, 22, 23, and 25) were individually fitted with a third-order polynomial to judge the degree of variation amongst the antennas. The results are shown in Fig. 8

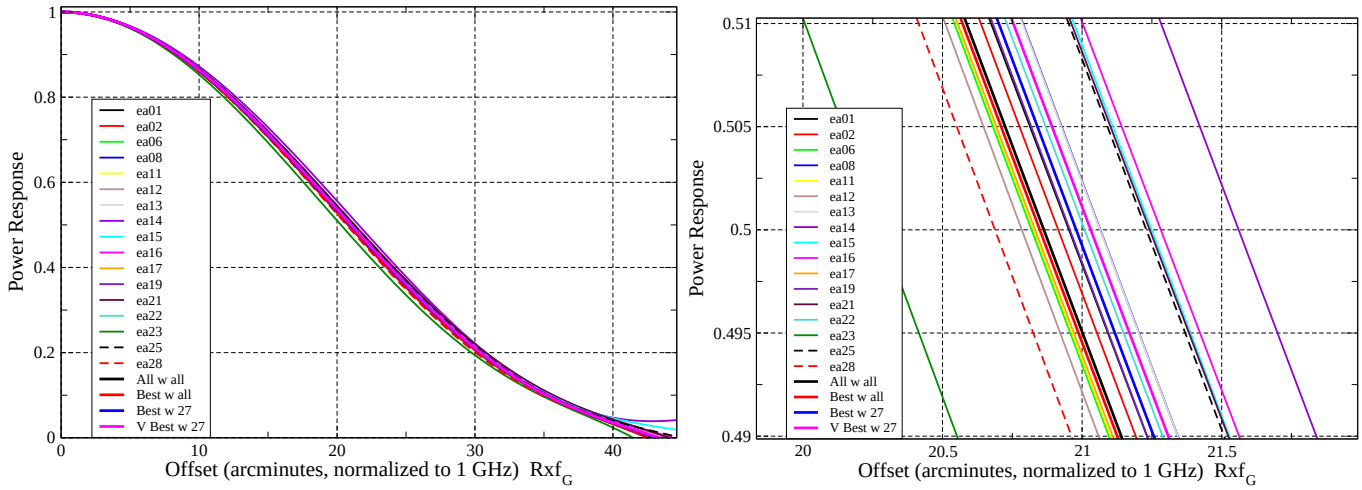

Figure 8: The variation in beam shape amongst 17 VLA antennas at 2948 MHz. The right panel is a zoom-in of the half-power region. Antennas 23 and 19 are clearly discrepant, and have been excluded from the global average. The power variation amongst the remaining antennas has a maximum ∼2% spread at the half-power point.

The nine antennas at the center of the preceding plot were then utilized to form the 'global mean' response for each spectral window, using a single reference antenna and averaging over the central 54 Mhz of each window. The results are shown in Fig. 9. An important result from this is that the primary beams (after correction for

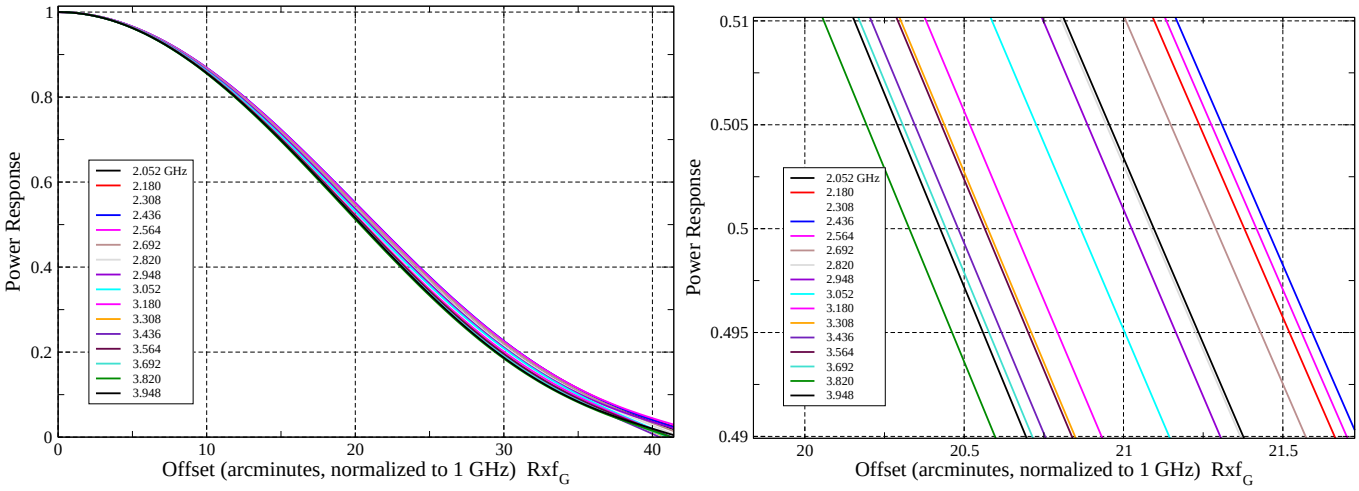

Figure 9: The variation in beam shape as a function of frequency across S-band. The right panel is a zoom-in of the central region, and clearly shows that the (normalized) half-width of the primary beam becomes steadily narrower as the frequency increases.

diffraction) become increasingly narrower at the high frequency end of the band. This result is consistent with the antenna efficiency observations made by me and Bob Hayward, which showed that the antenna efficiencies increase with increasing frequency. The probable origin of this is in the illumination by the primary horn, which is likely more uniform across the aperture at the high frequency half than at the low frequency half.

Excellent fits were made using a third-order polynomial (in even powers). The coefficients are given in Table 4.

Table 4: **Polynomial Fits for S-Band**

Freq. MHz	A_0	A_2 $\times 10^{-3}$	A_4 $\times 10^{-7}$	A_6 $\times 10^{-10}$	HWHM	Freq. MHz	A_0	A_2 $\times 10^{-3}$	A_4 $\times 10^{-7}$	A_6 $\times 10^{-10}$	HWHM
2052	1.000	-1.429	7.52	-1.47	21.10	3052	1.000	-1.467	8.05	-1.70	20.87
2180	1.000	-1.389	7.06	-1.33	21.38	3180	1.000	-1.497	8.38	-1.80	20.66
2308						3308	1.000	-1.504	8.37	-1.77	20.58
2436	1.000	-1.377	6.90	-1.27	21.45	3436	1.000	-1.521	8.63	-1.88	20.49
2564	1.000	-1.381	6.92	-1.26	21.42	3564	1.000	-1.505	8.37	-1.75	20.57
2692	1.000	-1.402	7.23	-1.40	21.29	3692	1.000	-1.521	8.51	-1.79	20.44
2820	1.000	-1.433	7.62	-1.54	21.09	3820	1.000	-1.534	8.57	-1.77	20.33
2948	1.000	-1.433	7.46	-1.42	21.03	3948	1.000	-1.516	8.30	-1.66	20.43

Typical rms residual is 0.4%. Typical errors in the four coefficients are .002, .010, .15, and .06 in the units given in the table. The units for HWHM are Arcmin-GHz.

Specific notes for these data:

- Reference antennas were: 03, 05, 07, 18, 20, 26, and 27.
- Antenna 09 was out of the array
- Antennas 04 and 10 were taken out of service partway through the run, and are not utilized in the analysis.
- Antenna 24 gave no good data in LCP in spectral windows 1 through 8.
- SPW03 is heavily corrupted by RFI (Sirius/XM), and has not been utilized in the analysis.
- SPW02 has satellite RFI in channels 34 through 44.

- To correct for gain compression due to the nearby passage of Sirius satellite S3 near 12:25 IAT, the data have been corrected by using the switched power monitoring system for all SPWs.

Affected data are flagged.

4.3.1 Data Archive Location

The calibrated data are archived on the ftp server at:
/home/ftp/pub/staff/rperley/BeamHoloDat/SBand
At this location are:

- The complete databases in both 'FITTP' and 'FITAB' formats, with names **HOLO-FITxx.** where 'xx' is either 'AB' or TP'. These files have the calibration tables attached. Files with the calibration already applied have names **HOLO-FITxx-CAL.**
- The individually separated spectral windows in FITTP format. These are named **SHOLO-SPWnn**, where nn is the SPW number, from 01 through 16. Each is about 27 GB.
- Files containing the calibrated output from the program 'UVHOL', with names **SHOLO-UVHOL-BEST9-ALLREF-SPWnnpp01**. Here, 'nn' is the SPW number 01 through 16, and 'pp' is the polarization pair, RR, RL, LR, or LL'. Each file contains all 64 individual channel cross-correlations between the sum of all the reference antennas with the sum of the best nine pointing antennas. Each of these files is about 19 MB.

Additionally, the 'UVHOL' output files used for the analysis presented here have been stored on disk at
/users/rperley/BeamData/SBand/S-ffffpp01
where 'ffff' is the central frequency in MHz of the spectral window (given in Table 3), and 'pp' is the Stokes polarization RR, RL, LR, LL, I_, Q_, U_, or V_. The data are fully calibrated, averaged over the central 28 MHz of each spectral window, and are the average of the best nine centrally located pointed antennas (2, 11, 12, 13, 14, 15, 17, 22, and 24) with ea27, the central reference antenna.

4.4 C-Band

At this, and at all higher frequency bands, the beam observations were taken in a dual mode – an oversampled grid, typically 17 x 17 covering the central beam, and a much sparser grid, typically 23 x 23, extending out to the 4th null. The results below are taken from the central grid only.

Following the procedures outlined above, beam fits for each antenna at the central SPWs at 4948 and 6948 MHz were made to determine the range of behavior, and to identify well-behaved antennas. These were then utilized for determining the beam profiles as a function of frequency.

In Figure 10, I show the 'closeup' views of the beam shape distribution over antennas for 4948 (left) and 6948 MHz (right). In Figure 11 is shown the fits for all 32 spectral windows, utilizing the best-behaved antennas identified above. The thick dot-dash line is the beam profile described by the 2000 beam measurements, using the old VLA feed, taken in 2000 at 4885 MHz. The old and new profiles – at this frequency – are essentially identical. At this band, as at S-band, the normalized beamwidth becomes narrower in the upper half of the band. And, as at S-band, antenna efficiency measurements (on ea24) show the antenna efficiency is higher in this same frequency range than the lower half. For this case, I have direct evidence of the cause – dish holography has clearly showed that the illumination above 6 GHz is much more uniform than at 5 GHz.

The best 15 antennas were then used with a single reference antenna to generate the data used by PBEAM to measure the median profiles for all spectral windows. The results from these fits are given in Table 5.

Specific notes for these data:

- Out of the array : Antenna 01
- Reference antennas were: 02, 03, 07, 12, 14, 24, and 26
- No specific spectral flagging was necessary. All included antennas worked well.

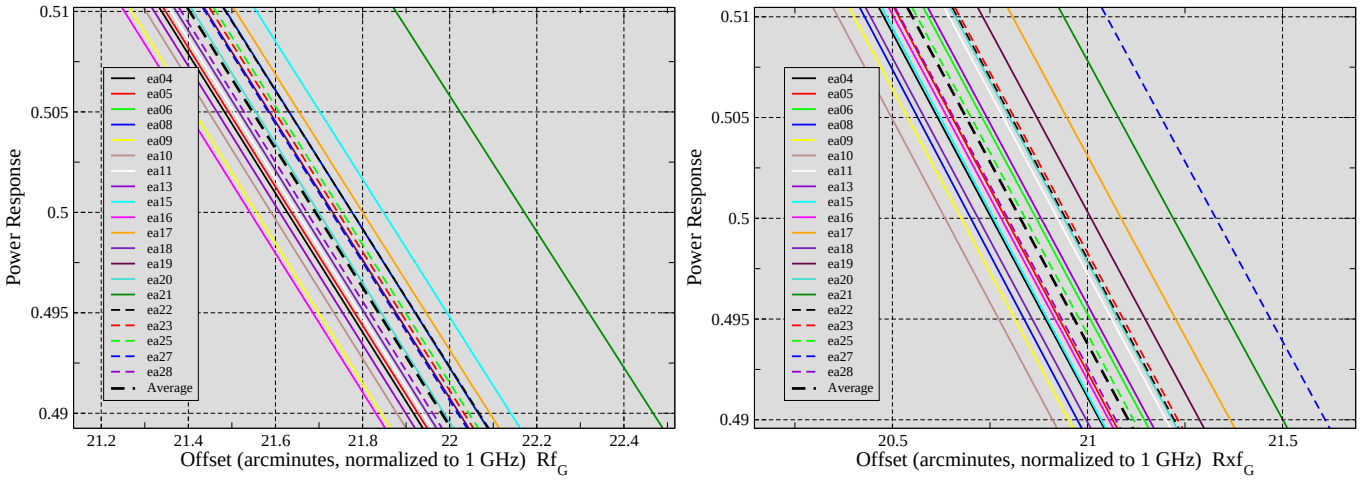

Figure 10: The variation in beam shape amongst 20 VLA antennas at 4948 MHz (left) and 6948 MHz (right). The power variation amongst the remaining antennas has a maximum ∼2.5% spread at the half-power point.

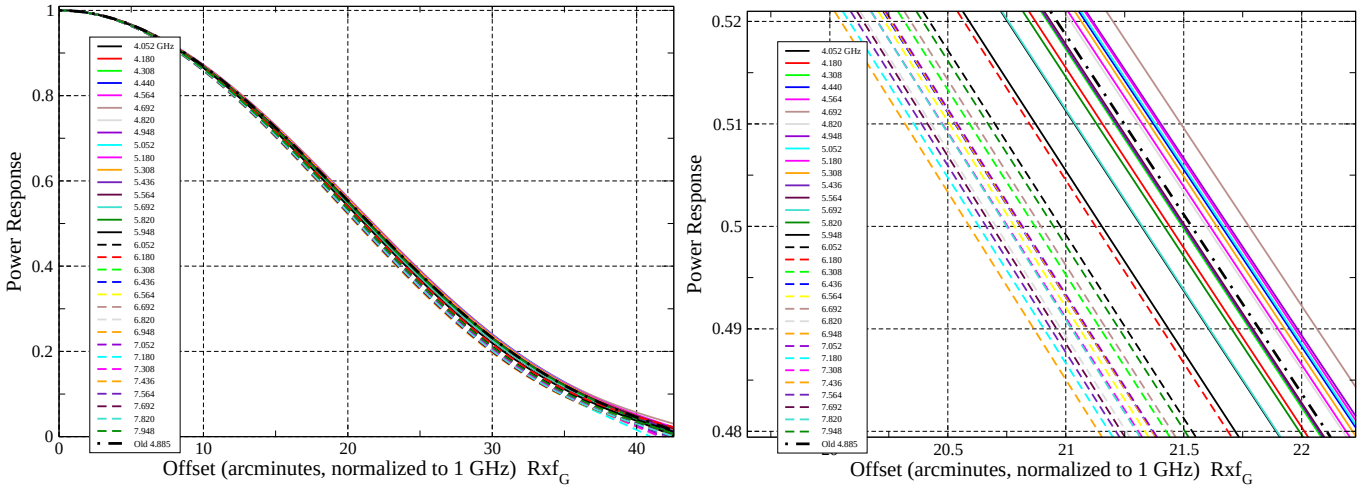

Figure 11: The variation in beam shape as a function of frequency across C-band. The high-frequency half of the spectral windows are shown in dashed lines. The right panel is a zoom-in of the central region, and clearly shows that the (normalized) half-width of the primary beam becomes steadily narrower as the frequency increases. The thick dot-dash line shows the beam profile at 4885 MHz for the old VLA.

4.4.1 Data Archive Location

The two calibrated databases (one from each day, corresponding to the lower and upper halves of the band) have been archived on the ftp server at:
/home/ftp/pub/staff/rperley/BeamHoloDat/CBand/CHOLO-yy-FITxx
in both 'FITTP' and 'FITAB' formats, where 'xx' is either 'AB' or TP', and 'yy' is 'LO' or 'HI'. The files are about 150 GB. These have the calibration tables attached. Versions with the calibration already applied are at:
/home/ftp/pub/staff/rperley/BeamHoloDat/CBand/CHOLO-yy-FITxx-CAL
in both 'FITTP' and 'FITAB' formats, where 'xx' is either 'AB' or TP', and 'yy' is 'LO' or 'HI'.

The 'UVHOL' output files used for the analysis presented here have been stored on disk at:
/users/rperley/BeamData/CBand/C-BEAM-ffffpp01
where 'ffff' is the central frequency in MHz of the spectral window (given in Table 5), and 'pp' is the Stokes polarization I_, Q_, U_, or V_, RR, RL, LR, LL. The data from the sparsely sampled grid is stored on disk at:
/users/rperley/BeamData/CBand/CW-BEAM-ffffpp01
, with the same meanings for 'ffff', and 'pp'. The data are fully calibrated, averaged over the central 28 MHz of each spectral window, and are the average of 14 pointing antennas (4, 5, 6, 8, 9, 11, 13, 16, 18, 19, 20, 22, 23,

Table 5: **Polynomial Fits for C-Band**

Freq. MHz	A_0	A_2 $\times 10^{-3}$	A_4 $\times 10^{-7}$	A_6 $\times 10^{-10}$	HWHM	Freq. MHz	A_0	A_2 $\times 10^{-3}$	A_4 $\times 10^{-7}$	A_6 $\times 10^{-10}$	HWHM
4052	1.000	-1.406	7.41	-1.48	21.32	6052	1.000	-1.445	7.68	-1.50	20.98
4180	1.000	-1.385	7.09	-1.36	21.44	6148	1.000	-1.422	7.38	-1.38	21.13
4308	1.000	-1.380	7.08	-1.37	21.50	6308	1.000	-1.463	7.94	-1.62	20.88
4436	1.000	-1.362	6.95	-1.35	21.65	6436	1.000	-1.478	8.22	-1.74	20.82
4564	1.000	-1.365	6.92	-1.31	21.62	6564	1.000	-1.473	8.00	-1.62	20.79
4692	1.000	-1.339	6.56	-1.17	21.78	6692	1.000	-1.455	7.76	-1.53	20.91
4820	1.000	-1.371	7.06	-1.40	21.60	6820	1.000	-1.487	8.22	-1.72	20.71
4948	1.000	-1.358	6.91	-1.34	21.70	6948	1.000	-1.472	8.05	-1.67	20.82
5052	1.000	-1.360	6.91	-1.33	21.68	7052	1.000	-1.470	8.01	-1.64	20.80
5180	1.000	-1.353	6.74	-1.25	21.70	7180	1.000	-1.503	8.50	-1.84	20.64
5308	1.000	-1.359	6.82	-1.27	21.64	7308	1.000	-1.482	8.19	-1.72	20.76
5436	1.000	-1.380	7.05	-1.37	21.51	7436	1.000	-1.498	8.22	-1.66	20.60
5564	1.000	-1.376	6.99	-1.31	21.51	7564	1.000	-1.490	8.18	-1.66	20.67
5692	1.000	-1.405	7.39	-1.47	21.33	7692	1.000	-1.481	7.98	-1.56	20.69
5820	1.000	-1.394	7.29	-1.45	21.42	7820	1.000	-1.474	7.94	-1.57	20.75
5948	1.000	-1.428	7.57	-1.57	21.16	7948	1.000	-1.448	7.69	-1.51	20.95

Typical rms in the fit was 0.5%. Typical errors in the coefficients are .003, .021, .38, and .19 in the units given in the table. The units of the HWHM are Arcmin-GHz.

25) with a single reference antenna, ea28.

4.5 X-Band

As at C-band, the full bandwidth was covered in two observing runs, the first for the lower half, the second for the upper half. Following the procedures outline above, beam fits for each antenna at the central SPWs at 8948 and 10948 MHz were made to determine the range of behavior, and to identify well-behaved antennas. These were then utilized for determining the beam profiles as a function of frequency.

In Figure 12, is shown the 'closeup' views of the spread of the power beam pattern over antennas for 8948 (left) and 10948 MHz (right). The maximum spread, disregarding the discrepant antennas (principally ea20) is 4%. In Figure 13 is shown the fits for all 32 spectral windows, using the central 34 MHz of each spectral

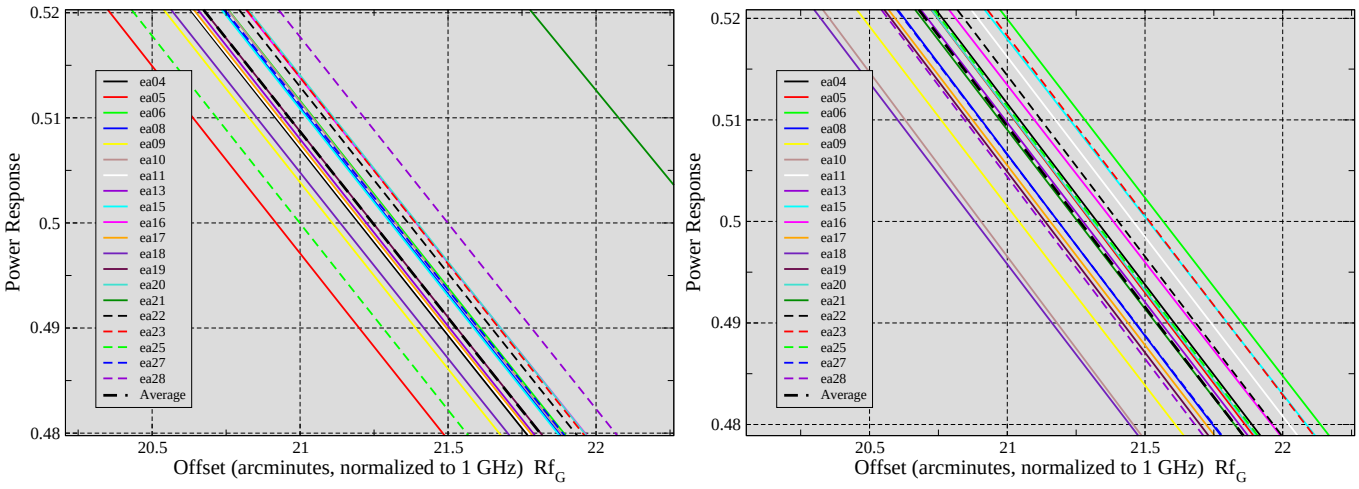

Figure 12: The variation in beam shape amongst 20 VLA antennas at 8948 MHz (left) and 10948 MHz (right). The power variation amongst the remaining antennas has a maximum ∼4% spread at the half-power point.

window, and the best-behaved antennas identified above. The thick dot-dash line shows the old VLA profile at 8435 MHz taken in 2000. The new feed evidently provides a more uniform illumination, resulting in a primary

beam $\sim$ 4% narrower than the old feed. The (normalized) beam shapes and beam widths across X-band are

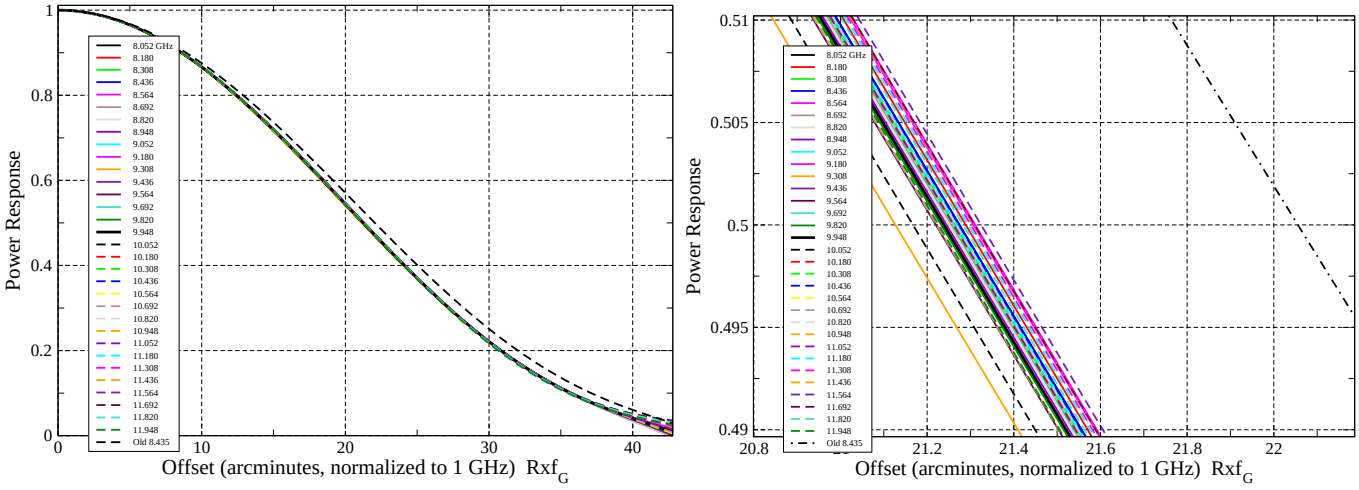

Figure 13: The variation in beam shape as a function of frequency across X-band. There is no evident trend for any change in beamwidth with frequency beyond that expected from diffraction. The thick dot-dash line shows the profile from the old VLA feed at 8435 MHz. The new feed provides a beam $\sim$ 4% narrower than the old.

much more uniform than at lower frequencies.

The data used to generate the average profiles shown above were then fitted with a 3rd order polynomial. For these fits, a single reference antenna with the best 14 moving antennas was used. The coefficients are given in Table 6.

Table 6: **Polynomial Fits for X-Band**

Freq. MHz	A_0	A_2 $\times 10^{-3}$	A_4 $\times 10^{-7}$	A_6 $\times 10^{-10}$	HWHM	Freq. MHz	A_0	A_2 $\times 10^{-3}$	A_4 $\times 10^{-7}$	A_6 $\times 10^{-10}$	HWHM
8052	1.000	-1.403	7.21	-1.37	21.28	10052	1.000	-1.421	7.46	-1.45	21.17
8180	1.000	-1.398	7.10	-1.32	21.29	10180	1.000	-1.409	7.25	-1.36	21.22
8308	1.000	-1.402	7.16	-1.35	21.26	10308	1.000	-1.402	7.13	-1.31	21.26
8436	1.000	-1.400	7.12	-1.32	21.28	10436	1.000	-1.399	7.09	-1.29	21.27
8564	1.000	-1.391	6.95	-1.25	21.31	10564	1.000	-1.413	7.37	-1.43	21.22
8692	1.000	-1.409	7.34	-1.49	21.26	10692	1.000	-1.412	7.34	-1.41	21.22
8820	1.000	-1.410	7.36	-1.45	21.25	10820	1.000	-1.401	7.12	-1.31	21.27
8948	1.000	-1.410	7.34	-1.43	21.25	10948	1.000	-1.401	7.12	-1.31	21.26
9052	1.000	-1.403	7.20	-1.36	21.27	10052	1.000	-1.401	7.12	-1.31	21.26
9180	1.000	-1.396	7.09	-1.31	21.31	11180	1.000	-1.394	6.99	-1.24	21.30
9308	1.000	-1.432	7.68	-1.55	21.13	11308	1.000	-1.394	7.01	-1.26	21.30
9436	1.000	-1.414	7.43	-1.47	21.24	11436	1.000	-1.391	6.94	-1.22	21.31
9564	1.000	-1.416	7.45	-1.47	21.22	11564	1.000	-1.389	6.92	-1.22	21.33
9692	1.000	-1.406	7.26	-1.39	21.26	11692	1.000	-1.386	6.80	-1.15	21.31
9820	1.000	-1.412	7.36	-1.43	21.24	11820	1.000	-1.391	6.88	-1.19	21.28
9948	1.000	-1.409	7.29	-1.39	21.24	11948	1.000	-1.399	6.97	-1.22	21.23

Typical rms residual in the fit is 0.7%. Typical 1σ errors in the coefficients are: .003, .019, .28, .12, in the units specified in the table. The units of the HWHM are Arcmin-GHz.

Specific notes for these data:

- Antenna out of the array: 01
- Reference antennas were: 02, 03, 07, 12, 14, 24, and 26.
- No specific spectral flagging was necessary. All included antennas worked well.

4.5.1 Data Archive Location

The two calibrated databases (one from each day, corresponding to the lower and upper halves of the band) have been archived on the ftp server at:
/home/ftp/pub/staff/rperley/BeamHoloDat/XBand/XHOLO-yy-FITxx
in both 'FITTP' and 'FITAB' formats, where 'xx' is either 'AB' or TP', and 'yy' is 'LO' or 'HI'. The files are about 120 GB each. These have the calibration tables attached. Versions with the calibration already applied are at:
/home/ftp/pub/staff/rperley/BeamHoloDat/CBand/XHOLO-yy-FITxx-CAL
in both 'FITTP' and 'FITAB' formats, where 'xx' is either 'AB' or TP', and 'yy' is 'LO' or 'HI'.

The 'UVHOL' output files used for the analysis presented here have been stored on disk at:
/users/rperley/BeamData/XBand/X-ffffpp01,
where 'ffff' is the central frequency in MHz of the spectral window (given in Table 6), and 'pp' is the Stokes polarization I_, Q_, U_, or V_, RR, RL, LR, LL. The data from the sparsely sampled grid is stored on disk at:
/users/rperley/BeamData/XBand/XW-ffffpp01
, with the same meanings for 'ffff', and 'pp'. The data are fully calibrated, averaged over the central 28 MHz of each spectral window, and are the average of the best 14 pointed antennas (4, 8, 9, 10, 11, 13, 15, 16, 18, 19, 20, 21, 22, 23) with the reference antennas (3, 12, 24 and 26).

4.6 Ku-Band

Observations for this band were taken on three dates, spanning the lower, middle, and upper 2GHz of the bandpass. Following the procedures outline above, beam fits for each antenna at the central SPWs at 12948, 14948, and 16948 MHz were made to determine the range of behavior, and to identify well-behaved antennas. These were then utilized for determining the beam profiles as a function of frequency.

In Figure 14, I show the 'closeup' views of the beamshape spread over antennas for 12948 (left) 14948 (middle) and 16948 MHz (right). In Figure 15 is shown the fits for all 48 spectral windows. For these all seven reference

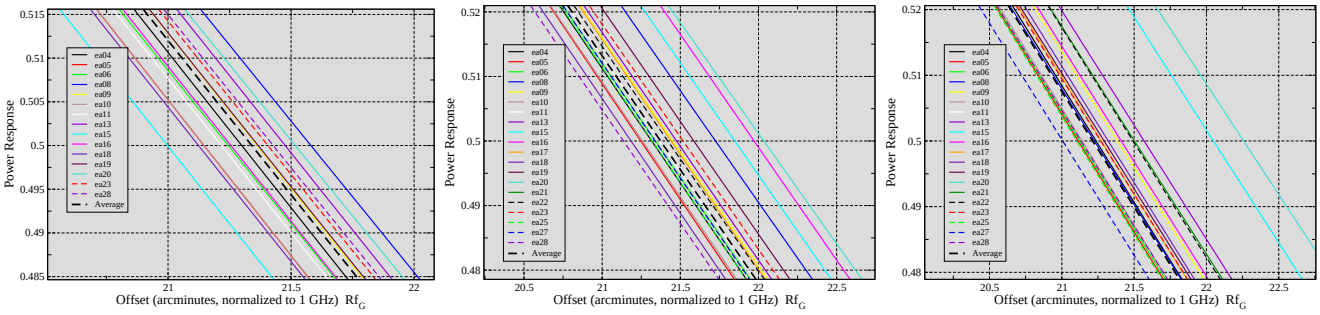

Figure 14: The variation in beam shape amongst 16 VLA antennas at 12948 MHz (left) 14948 MHz (middle) and 16948 MHz (right). The power variation amongst the best 14 antennas has a maximum ∼4% spread at the half-power point.

antennas were summed against the sum of the best 14 target antennas, using the central 34 MHz of each spectral window. The thick dot-dash line is the profile generated at 14965 MHz from the old VLA feed – it is ∼3% wider than the current beam at that frequency. There is a significant narrowing of the beam – by about 1% – towards the upper end of the band.

The data used to generate the average profiles shown above were then fitted with a 3rd order polynomial. The coefficients are given in Table 7.

Specific notes for these data:

- Antenna 01 was out of the array for all three observations. In addition, antenna 12 was out for the low frequency observation.
- Reference antennas were: 02, 03, 07, 12, 14, 24, and 26.
- There is considerable RFI seen in the short spacings for spectral windows 2 through 7 in the low frequency data (12.1 – 12.7 GHz). However, the longer spacings have sufficient fringe rate that the data are not significantly impacted for beam fitting purposes.

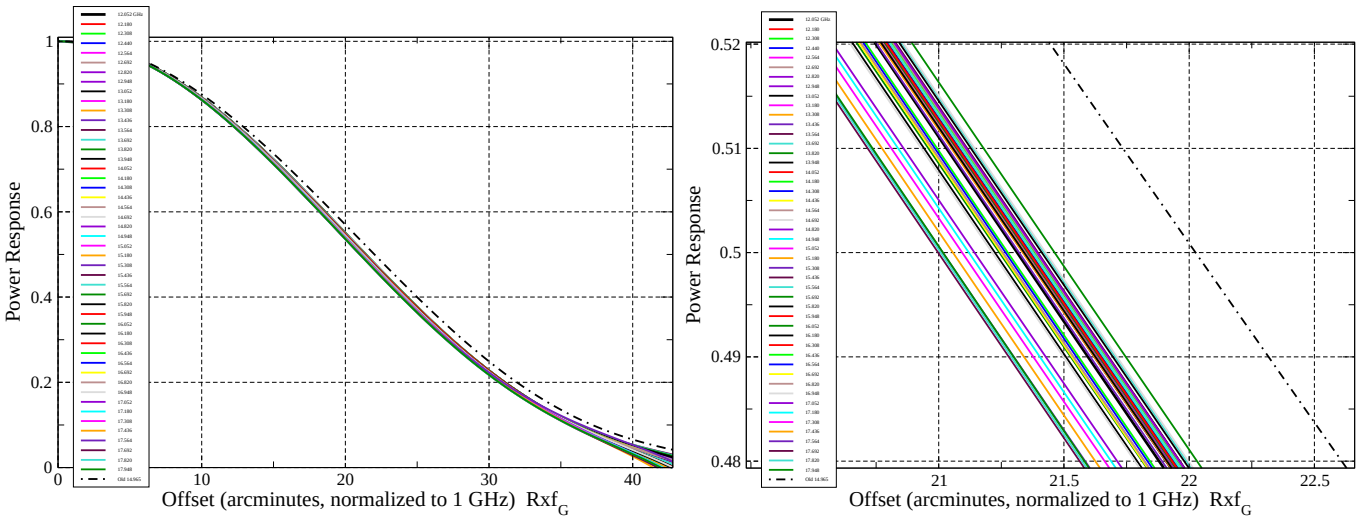

Figure 15: The variation in beam shape as a function of frequency across Ku-band. The right panel is a zoom-in of the central region. The thick dot-dash line shows the old VLA beam at 14965 MHz. The new feed generates a beam ∼3% narrower than the old feed at this frequency.

- All antennas performed well.

4.6.1 Data Archive Location

The three calibrated databases (one from each day, corresponding to the lower middle, and upper 2 GHz portions of the band) have been archived on the ftp server at:
/home/ftp/pub/staff/rperley/BeamHoloDat/UBand/KU-yyy-FITxx
in both 'FITTP' and 'FITAB' formats, where 'xx' is either 'AB' or TP', and 'yyy' is 'LOW' 'MID' or 'HI'. The files are about 110 GB. These have the calibration tables attached. Versions with the calibration already applied are at:
/home/ftp/pub/staff/rperley/BeamHoloDat/CBand/KU-yyy-FITxx-CAL
in both 'FITTP' and 'FITAB' formats, where 'xx' is either 'AB' or TP', and 'yy' is 'LO' or 'HI'.

The 'UVHOL' output files used for the analysis presented here have been stored on disk at:
/users/rperley/BeamData/UBand/U-ffffpp01,
where 'ffff' is the central frequency in MHz of the spectral window (given in Table 7), and 'pp' is the Stokes polarization I_, Q_, U_, or V_, RR, RL, LR, LL. The data from the sparsely sampled grid is stored on disk at:
/users/rperley/BeamData/UBand/UW-ffffpp01
, with the same meanings for 'ffff', and 'pp'. The data are fully calibrated, averaged over the central 28 MHz of each spectral window, and are the average of the best pointed antennas (4, 5, 9, 10, 11, 13, 16, 17, 18, 19, 20, 21, 23) with the average of all 7 reference antennas (2, 3, 7, 12, 24, 26).

4.7 K-Band

At this, and the two higher frequency bands, there was not enough available time to survey the full frequency span. At this band, which has a full bandwidth of ∼8 GHz, I surveyed the primary beams in every other 1-GHz-wide span. Following the procedures outlined above, beam fits for each antenna at the central SPWs at 19564 and 23052 MHz were made to determine the range of behavior, and to identify well-behaved antennas. These were then utilized for determining the beam profiles as a function of frequency.

In Figure 16, I show the 'closeup' views of the spread over antennas for 19564 (left) and 23052 MHz (right). From this the best eleven antennas were identified, and the data from the sum of these against a single reference antenna utilzed to fit the primary beams for all 32 spectral windows, as shown in Figure 17.

The data used to generate the average profiles shown above were then fitted with a 3rd order polynomial. The coefficients are given in Table 8.

Specific notes for these data:

- Antenna 01 was out of the array for both observations. Antenna 25 was out for the high frequency observation.

Table 7: **Polynomial Fits for Ku-Band**

Freq. MHz	A_0	A_2 $\times 10^{-3}$	A_4 $\times 10^{-7}$	A_6 $\times 10^{-10}$	HWHM	Freq. MHz	A_0	A_2 $\times 10^{-3}$	A_4 $\times 10^{-7}$	A_6 $\times 10^{-10}$	HWHM
12052	1.000	-1.399	7.17	-1.34	21.32	15052	1.000	-1.402	7.38	-1.48	21.35
12180	1.000	-1.392	7.07	-1.31	21.35	15180	1.000	-1.407	7.47	-1.53	21.34
12308	1.000	-1.393	7.19	-1.38	21.39	15308	1.000	-1.406	7.41	-1.48	21.32
12436	1.000	-1.393	7.20	-1.40	21.39	15436	1.000	-1.399	7.31	-1.44	21.36
12564	1.000	-1.395	7.19	-1.38	21.36	15564	1.000	-1.397	7.28	-1.43	21.38
12692	1.000	-1.397	7.20	-1.37	21.35	15692	1.000	-1.401	7.35	-1.46	21.36
12820	1.000	-1.388	7.06	-1.32	21.39	15820	1.000	-1.402	7.34	-1.45	21.34
12948	1.000	-1.397	7.18	-1.36	21.34	15948	1.000	-1.399	7.30	-1.44	21.36
13052	1.000	-1.400	7.27	-1.40	21.34	16052	1.000	-1.419	7.59	-1.54	21.24
13180	1.000	-1.406	7.44	-1.50	21.34	16180	1.000	-1.419	7.59	-1.52	21.22
13308	1.000	-1.403	7.37	-1.47	21.34	16308	1.000	-1.412	7.40	-1.44	21.25
13436	1.000	-1.392	7.08	-1.31	21.36	16436	1.000	-1.407	7.32	-1.40	21.28
13564	1.000	-1.384	6.94	-1.24	21.40	16564	1.000	-1.408	7.32	-1.41	21.27
13692	1.000	-1.382	6.95	-1.25	21.42	16692	1.000	-1.410	7.34	-1.40	21.25
13820	1.000	-1.376	6.88	-1.24	21.46	16820	1.000	-1.407	7.27	-1.38	21.26
13948	1.000	-1.384	6.98	-1.28	21.41	16948	1.000	-1.423	7.63	-1.55	21.21
14052	1.000	-1.400	7.36	-1.48	21.37	17052	1.000	-1.437	7.87	-1.66	21.14
14180	1.000	-1.397	7.29	-1.45	21.38	17180	1.000	-1.438	7.84	-1.64	21.12
14308	1.000	-1.399	7.32	-1.45	21.36	17308	1.000	-1.445	7.98	-1.71	21.09
14436	1.000	-1.396	7.25	-1.42	21.38	17436	1.000	-1.452	8.10	-1.77	21.06
14564	1.000	-1.393	7.20	-1.39	21.39	17564	1.000	-1.458	8.13	-1.70	21.02
14692	1.000	-1.384	7.03	-1.31	21.43	17692	1.000	-1.456	8.06	-1.72	21.00
14820	1.000	-1.388	7.06	-1.32	21.39	17820	1.000	-1.453	8.00	-1.68	21.01
14948	1.000	-1.393	7.16	-1.37	21.37	17948	1.000	-1.452	7.99	-1.69	21.02

Typical rms residual is 0.7%. Typical errors in the coefficients are .004, .021, .30, .12 in the same units as given in the table. The units of the HWHM are Arcmin-GHz.

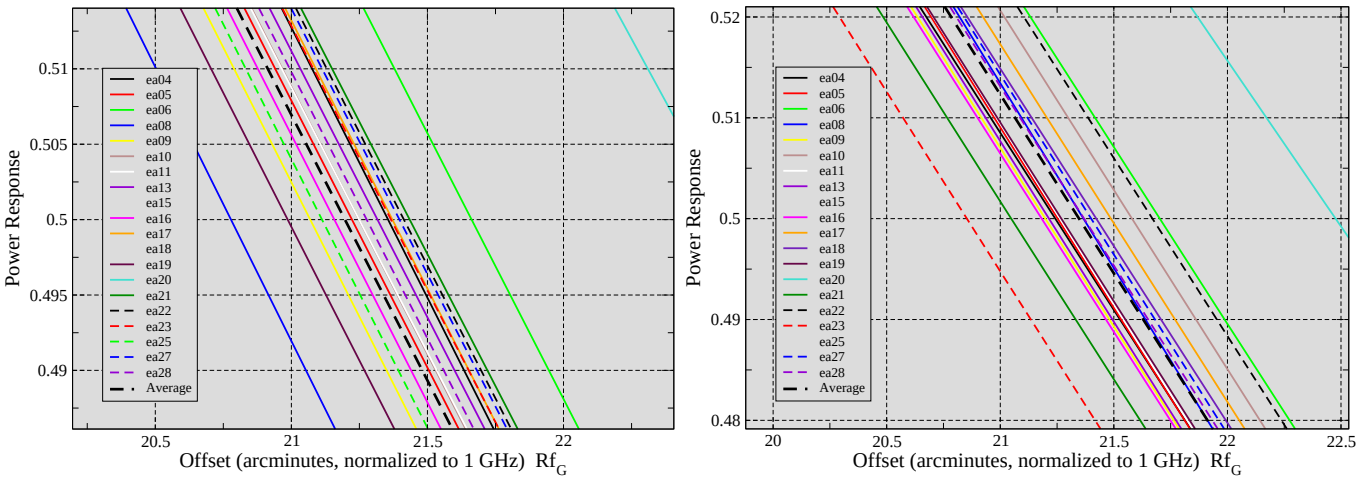

Figure 16: The variation in beam shape amongst 20 VLA antennas at 19564 MHz (left) and 23052 MHz (right). The power variation amongst the better-behaved antennas has a maximum ∼3.5% spread at the half-power point.

- Reference antennas were: 02, 03, 07, 12, 14, 24, and 26.
- Some antennas wandered away from the correct pointing position in the hour-long span between referenced pointings. Antennas notably affected are ea18, ea25, ea8, and ea15 for the 'LO' frequency, and ea08, ea15, ea16, and ea24 in the 'HI' data.

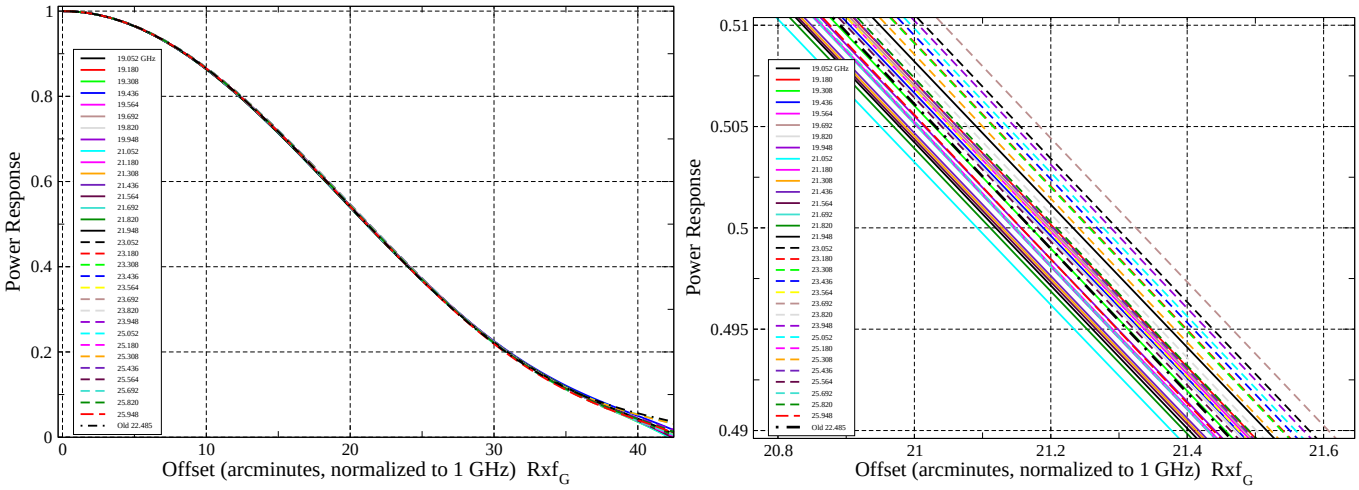

Figure 17: The variation in beam shape as a function of frequency across K-band. The right panel is a zoom-in of the central region. There is about a 1% spread in deviation of half-power width from the expected diffraction dependence, with no believable trend with frequency.

- All antennas performed well.

4.7.1 Data Archive Location

The two calibrated databases (one from each day, corresponding to the lower and upper tunings) have been archived on the ftp server at:
/home/ftp/pub/staff/rperley/BeamHoloDat/KBand/KHOLO-yy-FITxx
in both 'FITTP' and 'FITAB' formats, where 'xx' is either 'AB' or TP', and 'yy' is 'LO' or 'HI'. The files are about 110 GB. These have the calibration tables attached. Versions with the calibration already applied are at:
/home/ftp/pub/staff/rperley/BeamHoloDat/CBand/KHOLO-yy-FITxx-CAL
in both 'FITTP' and 'FITAB' formats, where 'xx' is either 'AB' or TP', and 'yy' is 'LO' or 'HI'.

The 'UVHOL' output files used for the analysis presented here have been stored on disk at:
/users/rperley/BeamData/KBand/K-ffffpp01,
where 'ffff' is the central frequency in MHz of the spectral window (given in Table 8), and 'pp' is the Stokes polarization I_, Q_, U_, or V_, RR, RL, LR, LL. The data from the sparsely sampled grid is stored on disk at:
/users/rperley/BeamData/KBand/KW-ffffpp01
, with the same meanings for 'ffff', and 'pp'. The data are fully calibrated, averaged over the central 28 MHz of each spectral window, and are the average of the best pointed antennas (4, 6, 8, 9, 11, 13, 15 16 17 18 19 22 23 27 28) with the reference antennas (2, 3, 7, 12, 14, 24).

4.8 Ka-Band

As at K-band, we could not survey the entire band, so settled for spanning four GHz out of the 13 GHz, on two days. Having learned from the K-band observations that the antennas cannot hold position accurately enough for an hour following a referenced pointing, I decreased the interval between pointings to 20 minutes for this observation – this seems to have worked well.

Following the procedures outlined above, beam fits for each antenna at the central SPWs at 29948 and 31948 MHz were made to determine the range of behavior, and to identify well-behaved antennas. These were then utilized for determining the beam profiles as a function of frequency.

In Figure 18, we show the 'closeup' views of the spread over antennas for 29948 (left) and 31948 MHz (right). The variation in beamwidth at the half power is about about 7%. From this, the best 10 antennas were summed against a single antenna to generate the files utilized for fitting the beam parameters. In Figure 19 is shown the fits for all 32 spectral windows. There is little evidence of a variation in beam shape beyond that expected from diffraction.

The data used to generate the average profiles shown above were then fitted with a 3rd order polynomial. The coefficients are given in Table 9.

Table 8: **Polynomial Fits for K-Band**

Freq. MHz	A_0	A_2 $\times 10^{-3}$	A_4 $\times 10^{-7}$	A_6 $\times 10^{-10}$	HWHM	Freq. MHz	A_0	A_2 $\times 10^{-3}$	A_4 $\times 10^{-7}$	A_6 $\times 10^{-10}$	HWHM
19052	1.000	-1.419	7.56	-1.53	21.23	23052	1.000	-1.401	7.21	-1.37	21.30
19180	1.000	-1.426	7.70	-1.59	21.21	23180	1.000	-1.408	7.31	-1.41	21.26
19308	1.000	-1.433	7.82	-1.64	21.17	23308	1.000	-1.407	7.28	-1.39	21.26
19436	1.000	-1.429	7.73	-1.60	21.18	23436	1.000	-1.407	7.31	-1.41	21.27
19564	1.000	-1.427	7.70	-1.59	21.20	23564	1.000	-1.419	7.47	-1.47	21.20
19692	1.000	-1.425	7.65	-1.56	21.20	23692	1.000	-1.395	7.10	-1.33	21.33
19820	1.000	-1.430	7.76	-1.62	21.19	23820	1.000	-1.413	7.36	-1.42	21.22
19948	1.000	-1.434	7.81	-1.63	21.16	23948	1.000	-1.402	7.21	-1.36	21.29
21052	1.000	-1.448	8.05	-1.73	21.09	25052	1.000	-1.402	7.17	-1.31	21.28
21180	1.000	-1.436	7.84	-1.63	21.15	25180	1.000	-1.432	7.73	-1.58	21.15
21308	1.000	-1.441	7.94	-1.68	21.13	25308	1.000	-1.407	7.22	-1.33	21.24
21436	1.000	-1.439	7.89	-1.66	21.13	25436	1.000	-1.417	7.43	-1.45	21.20
21564	1.000	-1.442	7.96	-1.69	21.12	25564	1.000	-1.422	7.52	-1.48	21.18
21692	1.000	-1.435	7.81	-1.61	21.14	25692	1.000	-1.427	7.59	-1.52	21.15
21820	1.000	-1.442	7.92	-1.66	21.11	25820	1.000	-1.416	7.42	-1.44	21.21
21948	1.000	-1.439	7.82	-1.61	21.11	25948	1.000	-1.422	7.46	-1.45	21.16

Typical rms residual is 0.9%. Typical errors in the four coefficients are .005, .038, .41, and .17, in the units given in the table. The units of the FWHM are arcmin-GHz.

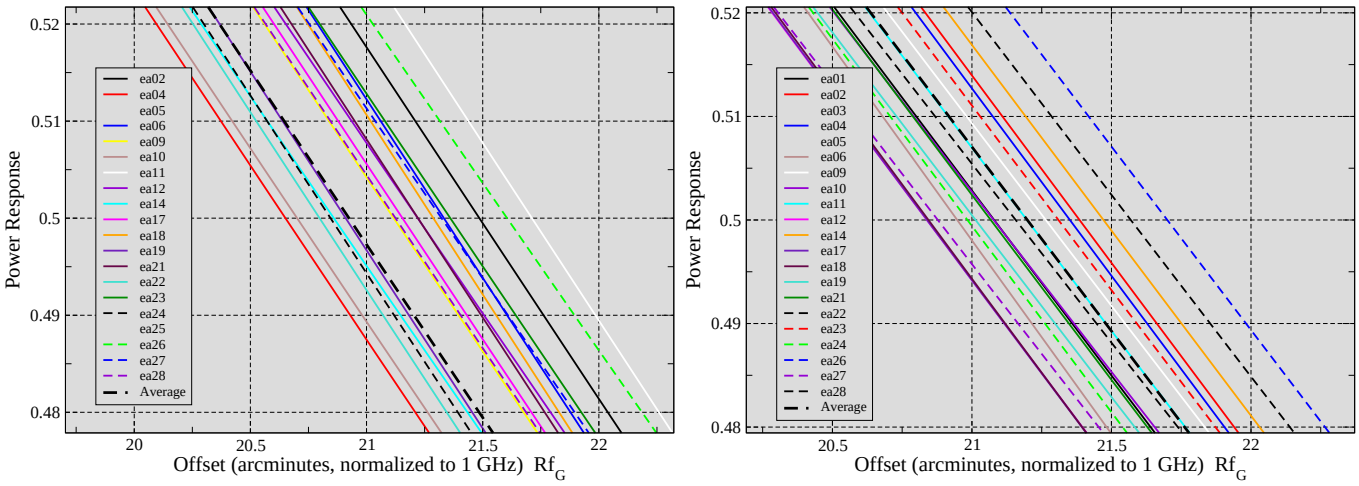

Figure 18: The variation in beam shape amongst 16 VLA antennas at 29948 MHz (left) and 31948 MHz (right). The power variation amongst the remaining antennas has a maximum ∼7% spread at the half-power point.

Specific notes for these data:

- Antenna 01 out of the array for the 'LO' obsrevations.
- Antennas out of the array for 'HI' observations were 03 and 25.
- Antenna 05 in RCP gave no data in the 'LO' observation, and gave no data in either polarization in the 'HI' observation.
- Antenna 25 failed referenced pointing for the 'LO' observations for the central beam part, and has not been utilized in the analysis.
- Reference antennas were: 03, 07, 08, 13, 15, 16, and 20.

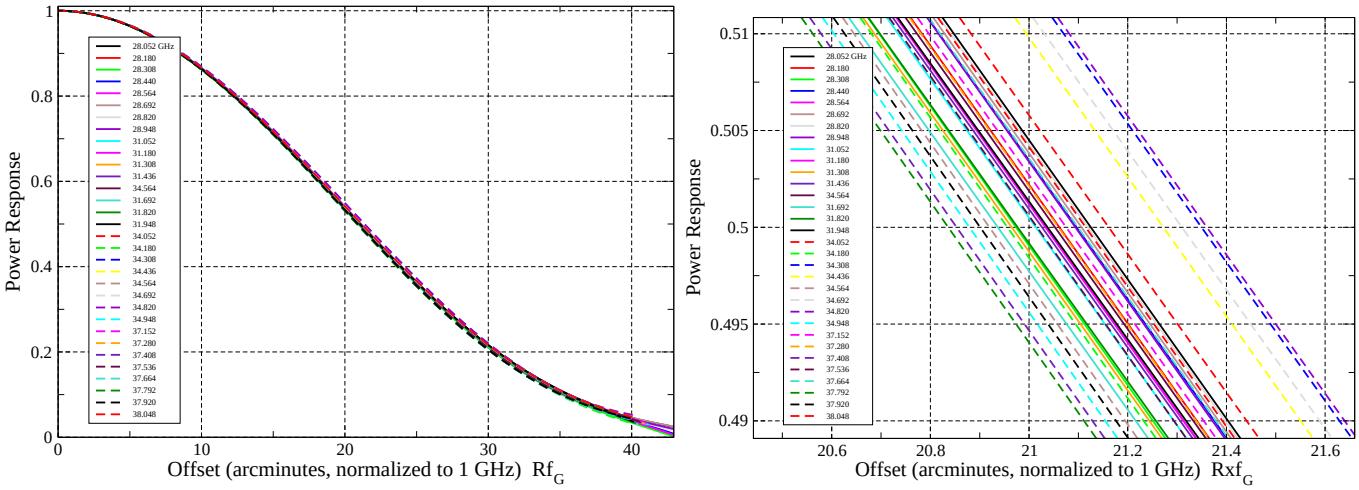

Figure 19: The variation in beam shape as a function of frequency across Ka-band. The variation across frequency is only ∼3%, with no believable trend in frequency.

4.8.1 Data Archive Location

The two calibrated databases (one from each day, corresponding to the lower and upper tunings) have been archived on the ftp server at:
/home/ftp/pub/staff/rperley/BeamHoloDat/ABand/AHOLO-yy-FITxx
in both 'FITTP' and 'FITAB' formats, where 'xx' is either 'AB' or TP', and 'yy' is 'LO' or 'HI'. The files are about 110 GB. These have the calibration tables attached. Versions with the calibration already applied are at:
/home/ftp/pub/staff/rperley/BeamHoloDat/CBand/AHOLO-yy-FITxx-CAL
in both 'FITTP' and 'FITAB' formats, where 'xx' is either 'AB' or TP', and 'yy' is 'LO' or 'HI'.

The 'UVHOL' output files used for the analysis presented here have been stored on disk at:
/users/rperley/BeamData/ABand/A-ffffpp01
where 'ffff' is the central frequency in MHz of the spectral window (given in Table 9), and 'pp' is the Stokes polarization I_, Q_, U_, or V_, RR, RL, LR, LL. The data from the sparsely sampled grid is stored on disk at:
/users/rperley/BeamData/ABand/AW-ffffpp01
with the same meanings for 'ffff', and 'pp'. The data are fully calibrated, averaged over the central 28 MHz of each spectral window, and are the average of the best pointed antennas (1 4 6 9 10 11 12 14 21 23 26) with the reference antennas (13, 15 20).

4.9 Q-Band

The Q-band observations were taken February 9, 2016, late at night, in excellent weather, using 3C84 at a good elevation. The low frequency pair (centered at 41.5 and 43.5 GHz) were taken first, the high frequency pair (46.5 and 48.5 GHz) next. Despite the uniformity of the weather throughout, the latter dataset could not be usefully employed for the beam measurements. In essence, no antennas showed a stable enough beam for proper polynomial fitting. The nominal half power widths determined for the higher frequency tuning pair were 10% larger than the lower frequency pair – there is no compelling argument to believe this is possible, since there is no tendency for the 43.5 GHz data to show a larger beam than the 41.5 GHz data.

Readers should note that it is extremely difficult for the VLA antennas to maintain and track position with the accuracy needed for beamshape measurements at this band. The grid spacing at the upper end of Q-band was 12 arcseconds. For an accurate measurement of beamshapes, errors in the grid points must be less than ∼10% of this – only 1.2 arcseconds! This means that the square grid pattern must hold to this precision over a duration of one hour. Evidently, the antennas were unable to do this for the high frequency portion of this observation.

However, the earlier half (lower frequency) of the observation gave sensible data, whose results are shown below.

In Figure 20, we show the beamshapes amongst the antennas at 41948 MHz (left), and a 'zoom-in' near the half-power (right). On the basis of the best 13 antennas, the median beam response was determined, using the

Table 9: **Polynomial Fits for Ka-Band**

Freq. MHz	A_0	A_2 $\times 10^{-3}$	A_4 $\times 10^{-7}$	A_6 $\times 10^{-10}$	HWHM	Freq. MHz	A_0	A_2 $\times 10^{-3}$	A_4 $\times 10^{-7}$	A_6 $\times 10^{-10}$	HWHM
28052	1.000	-1.444	7.61	-1.44	20.97	34052	1.000	-1.42	7.28	-1.34	21.08
28180	1.000	-1.439	7.54	-1.42	20.99	34180	1.000	-1.46	7.77	-1.53	20.89
28308	1.000	-1.457	7.87	-1.58	20.92	34308	1.000	-1.42	7.41	-1.42	21.09
28436	1.000	-1.457	7.90	-1.60	20.93	34436	1.000	-1.42	7.36	-1.39	21.10
28564	1.000	-1.455	7.87	-1.59	20.94	34564	1.000	-1.46	7.76	-1.52	20.87
28692	1.000	-1.458	7.88	-1.58	20.91	34692	1.000	-1.42	7.34	-1.38	21.08
28820	1.000	-1.453	7.81	-1.56	20.94	34820	1.000	-1.42	7.34	-1.39	21.15
28948	1.000	-1.460	7.98	-1.64	20.93	34948	1.000	-1.45	7.68	-1.49	20.90
31052	1.000	-1.415	7.44	-1.44	21.23	37152	1.000	-1.42	7.47	-1.44	21.15
31180	1.000	-1.408	7.26	-1.37	21.25	37280	1.000	-1.41	7.35	-1.40	21.21
31308	1.000	-1.413	7.28	-1.36	21.19	37408	1.000	-1.45	7.65	-1.46	20.94
31436	1.000	-1.394	7.07	-1.30	21.32	37536	1.000	-1.41	7.13	-1.29	21.22
31564	1.000	-1.404	7.23	-1.37	21.28	37664	1.000	-1.41	7.30	-1.38	21.26
31692	1.000	-1.427	7.48	-1.44	21.11	37792	1.000	-1.45	7.75	-1.50	20.92
31820	1.000	-1.418	7.48	-1.48	21.21	37820	1.000	-1.45	7.68	-1.49	20.99
31948	1.000	-1.413	7.37	-1.42	21.22	38048	1.000	-1.41	7.38	-1.43	21.27

Typical post-fit residual was 0.9%. Errors in the parameters are typically .004, .024, .36, and .16, in the same units as the table. The units of the HWHP are arcmin.GHz.

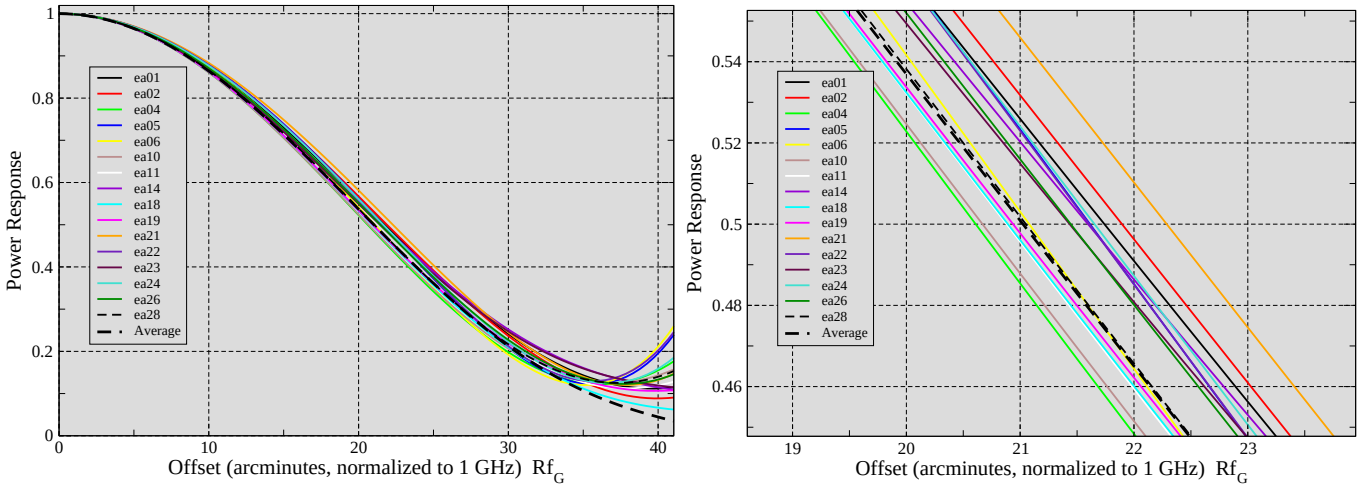

Figure 20: The variation in beam shape amongst 16 VLA antennas at 41948. The left panel shows the full function – the 'uplift' at low powers is not real, but likely a manifestation of low SNR. A zoom-in of the variation near the half-power point is shown in the right panel. The power variation amongst the remaining antennas has a maximum ∼12% spread at the half-power point.

average of these against two reference antennas. In Figure 21 is shown the fits for all 16 spectral windows in the lower half of Q-band.

The data used to generate the average profiles shown above were then fitted with a 3rd order polynomial. The coefficients are given in Table 10.

Specific notes for these data:

- Antennas out of the array were 9 and 25.
- Reference antennas: 03, 07, 08, 13, 15, 16, 20.
- All antennas exhibited significant deviations from the pointing needed for accurate beam determination.

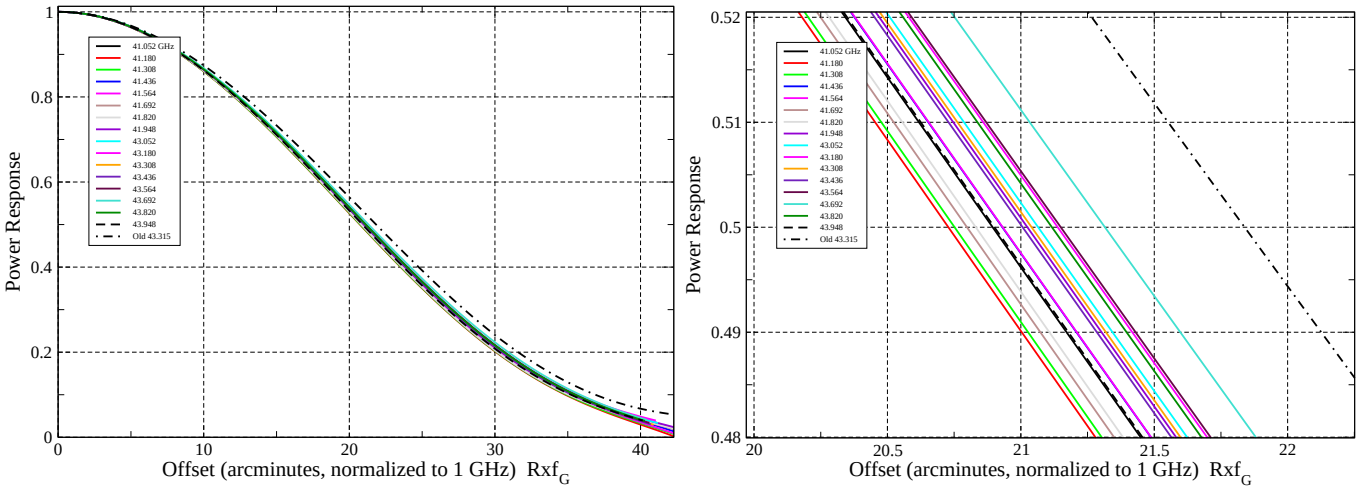

Figure 21: The variation in beam shape as a function of frequency across the lower half of Q-band. There is a spread of about 4%, which is likely dominated by measurement errors. The thick dot-dash line shows the beam profile measured in 2000 at 43.315 GHz. The current measurements indicate the beam is ∼4% smaller.

Table 10: **Polynomial Fits for Q-Band**

Freq. MHz	A_0	A_2 $\times 10^{-3}$	A_4 $\times 10^{-7}$	A_6 $\times 10^{-10}$	HWHM	Freq. MHz	A_0	A_2 $\times 10^{-3}$	A_4 $\times 10^{-7}$	A_6 $\times 10^{-10}$	HWHM
41052	1.000	-1.453	7.69	-1.47	20.89	43052	1.000	-1.428	7.40	-1.38	21.07
41180	1.000	-1.479	8.03	-1.61	20.73	43180	1.000	-1.418	7.29	-1.34	21.14
41308	1.000	-1.475	7.97	-1.58	20.75	43308	1.000	-1.433	7.49	-1.43	21.04
41436	1.000	-1.451	7.73	-1.51	20.93	43436	1.000	-1.438	7.55	-1.45	21.01
41564	1.000	-1.450	7.71	-1.51	20.93	43564	1.000	-1.419	7.36	-1.40	21.15
41692	1.000	-1.465	7.79	-1.49	20.80	43692	1.000	-1.397	7.13	-1.33	21.32
41820	1.000	-1.460	7.73	-1.47	20.83	43820	1.000	-1.423	7.39	-1.40	21.12
41948	1.000	-1.434	7.47	-1.40	21.02	43948	1.000	-1.452	7.68	-1.47	20.90

Typical post-fit rms is 1.6%. The typical estimated errors in the coefficients are .008, .045, .71, and .31, in the units given in the table. The units of the HWHP are arcmin.GHz.

4.9.1 Data Archive Location

The two calibrated databases (one from each day, corresponding to the lower and upper tunings) have been archived on the ftp server at:
/home/ftp/pub/staff/rperley/BeamHoloDat/QBand/QHOLO-yy-FITxx
in both 'FITTP' and 'FITAB' formats, where 'xx' is either 'AB' or TP', and 'yy' is 'LO' or 'HI'. The files are about 110 GB. These have the calibration tables attached. Versions with the calibration already applied are at:
/home/ftp/pub/staff/rperley/BeamHoloDat/CBand/QHOLO-LO-FITxx-CAL
in both 'FITTP' and 'FITAB' formats, where 'xx' is either 'AB' or TP'.

The 'UVHOL' output files used for the analysis presented here have been stored on disk at:
/users/rperley/BeamData/QBand/Q-ffffpp01,
where 'ffff' is the central frequency in MHz of the spectral window (given in Table 10), and 'pp' is the Stokes polarization I_, Q_, U_, V_, RR, RL, LR, LL. The data from the sparsely sampled grid is stored on disk at:
/users/rperley/BeamData/QBand/QW-ffffpp01
, with the same meanings for 'ffff', and 'pp'. The data are fully calibrated, averaged over the central 28 MHz of each spectral window, and are the average of the best pointed antennas (2 4 5 6 10 11 14 18 19 21 22 24 26) with two reference antennas (15, 20).

5 Comparisons and Discussion

5.1 VLA Beamwidths over Frequency

There are some significant variations in the normalized beamwidths over frequency, as shown in Fig. 22. The

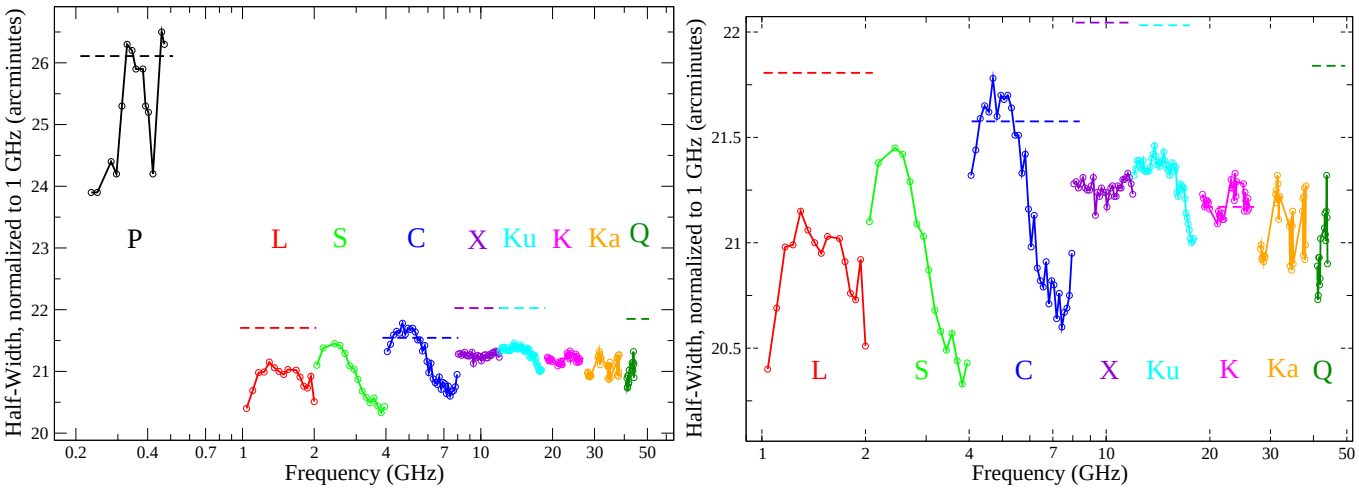

Figure 22: The variation of normalized width to the half-power as a function of frequency and band. (Left) All bands. The considerably wider half-width at P-band is due to the under-illumination of the primary reflector due to the dipole feed. (Right) The cassegrain feed bands. The significant trends at the lowest three bands are due to variations in the feed illumination. The short frequency scale variations at all bands probably reflect the uncertaintainties in the fits. Divide the values by the frequency in GHz to get the HWHP.

left panel shows all the bands on the same normalized scale. The reality of the large variations at P-band are difficult to judge, as the presence of the large 'plateau' is difficult to fit with a simple polynomial. The right panel is a zoom-in of the Cassegrain bands. Here there are clear trends in the beam widths at the lowest three bands that are certainly real.

The narrowing of the L-band beam at the low-frequency end is due to the over-illumination of the subreflector by the undersized feed. This situation was necessitated by the requirement for full frequency coverage from 1 to 50 GHz by the Expanded Very Large Array Project combined with the need to retain the original VLA subreflector. At S and C bands, there is a clear trend for steadily narrowing primary beams with increasing frequency, a consequence of a more uniform illumination of the primary by the feed with increasing frequency. This is supported by measurements by Perley and Hayward showing increasing antenna efficiency (for ea24) with increasing frequency, and by early dish holography directly showing a more uniform illumination in the upper half of C-band than at the lower half.

The beamwidth measurements at the five high frequency bands show a remarkably uniform width, with the likely exception of a small trend towards small beamsize at the upper end of Ku-band. The rapid variations in frequency of the beam width at K, Ka, and Q bands are likely due to noise or environmentally-induced variations, as the SNR is much lower, while the difficulty in holding position with the antennas much greater than at the other bands. It is also to be noted that the frequency coverage for these three bands is not continuous, so it is not possible to fairly judge whether some of the apparent jumps in width are real or not. For this reason, it may be best that beam width corrections for these bands not track these variations – a simple average is likely the safest course to take.

5.2 VLA vs Jansky VLA

The EVLA Project replaced the existing Cassegrain feeds at L, C, X, and Ku bands with newer wide-band designs. The existing feeds at P, K and Q bands were retained. Fig. 22 shows the comparison in beam widths between the old (horizontal dashed lines) and the newly measured ones. As expected, the measured beamwidths at P and K bands are unchanged from the old values (taken at the same frequency). This gives us some confidence that the methodology is repeatable. However, at Q-band, there is a significant difference, with the new measurements

being about 3.5% smaller than the old. I am inclined to believe that the newer measurements are correct, since the normalized beamwidths (∼20.7 arcmin-GHz) are comparable to other higher frequency bands. As noted earlier, it is very difficult to obtain a reliable measure of the beam at Q-band accurate to 5%.

The L, X, and Ku band beams are all narrower than their old VLA equivalents, typically by ∼3.5%. This must reflect a designed taper which puts more emphasis on the outer regions of the antenna surface. Surprisingly, the C-band beamwidth is exactly the same as it was in pre-VLA days.

6 Polarization

All data taken in this program – except at P-band – have been calibrated for polarization. Here I briefly discuss the results of examining the polarized beams for the Cassegrain-fed bands.

6.1 Stokes I and V

Images of the I and V antenna responses for each of the eight Cassegrain bands are shown in Fig. 23. The 'I' and 'V' images have been generated using slightly different methods for the sake of presentation. The 'I' beams are formed by gridding the Stokes 'I' visibilities: $I = (R + L)/2$, where 'R' and 'L' are the visibilities in the two oppositely polarized channels. Strictly speaking, the 'V' image should be formed from the difference: $V = (R - L)/2$. However, the amplitude of this result is (of course) always positive, and the sense of the Stokes 'V' polarization is seen in the phase – the 'LCP' lobe has a phase near 180 degrees, the 'RCP' lobe near 0. For presentation purposes, it is preferable to encode this phase into the amplitude – this has been done for Figure 23 by subtracting the LCP beam amplitude image from the RCP beam amplitude image – negative amplitudes now represent LCP, positive amplitude RCP. Note that these two different ways of representing the polarization beams are not the same. The images shown have zero phase – this is not in fact correct, as the 'RCP' and 'LCP' beams are complex – there are (small, but real) phase errors present in these beams, mostly due to errors in the optics. The most significant of these is any residual focus error, which imprints a radial phase gradient. Since no two antennas can be expected to have an identical focus errors, visibilities from sources off the pointing axis will have in general non-zero phases in their 'I' (and 'R' and 'L') visibilities. A proper correction algorithm must take these effects into account.

Immediately apparent in Figure 23 is the well-known 'squint' in the VLA's primary beams. The RCP and LCP beams (corresponding to the two polarization) are separated by a small angle, roughly equal to $2.4/\nu_G$ arcminutes, along an angle orthogonal to that joining the feed to the antenna axis. The relations are nicely shown in Figure 24. The top panel of the figure shows that the scaled separation of the RCP and LCP beams is nearly constant across all bands, equal to about 2.4 arcmin.GHz. There is good evidence that the squint is slightly larger at L-band than the others. The lower panel shows the position angle on the sky of the squint axis, with respect to the nominal position angle of the Cassegrain feed's position angle on the feed ring. The squint position angle is defined from RCP to LCP – the plot shows that all the VLA's circularly polarized feeds are defined identically, such that when the viewer is behind the antenna, and oriented along the line from the feed to the dish center, the RCP beam is on the right side, and the LCP is on the left, with a separation $\theta = 2.4/\nu_G$ arcminutes. Most of the scatter in these plots reflects the errors (chiefly from thermal noise) in the data. (Most of the outliers are due to RFI). The average position angle over each band should be 90 degrees – it is clear that Ku-band is about 3 degrees low, and K-band about 5 degrees high. The simplest explanation is that the position angle of these two feeds is off by the listed amounts from the fiducial values.

6.2 Stokes Q and U

The linear polarization characteristics are expected to show a radial orientation within the beam, rising from zero at the center to a few percent at the half power, and increasing (in fractional value) outwards. The images made show general agreement with this – the 'Q' images show a cloverleaf pattern, oriented along the quadrped legs, the 'U' images show the same pattern, rotated by 45 degrees. However, many images are highly distorted, and virtually all of them show phases which are far from the expected 0 or 180 degrees. In all cases, the phase difference between adjacent 'lobes' is 180 degrees, as expected – the problem is that they are not near the expected values. The apparent phase 'error' is not constant with frequency, nor is it the same between the 'Q' and 'U' images at the same frequency!

Fundamentally, this means that the RL and LR visibilities are not complex conjugates, as they should be for point source at the phase tracking center.

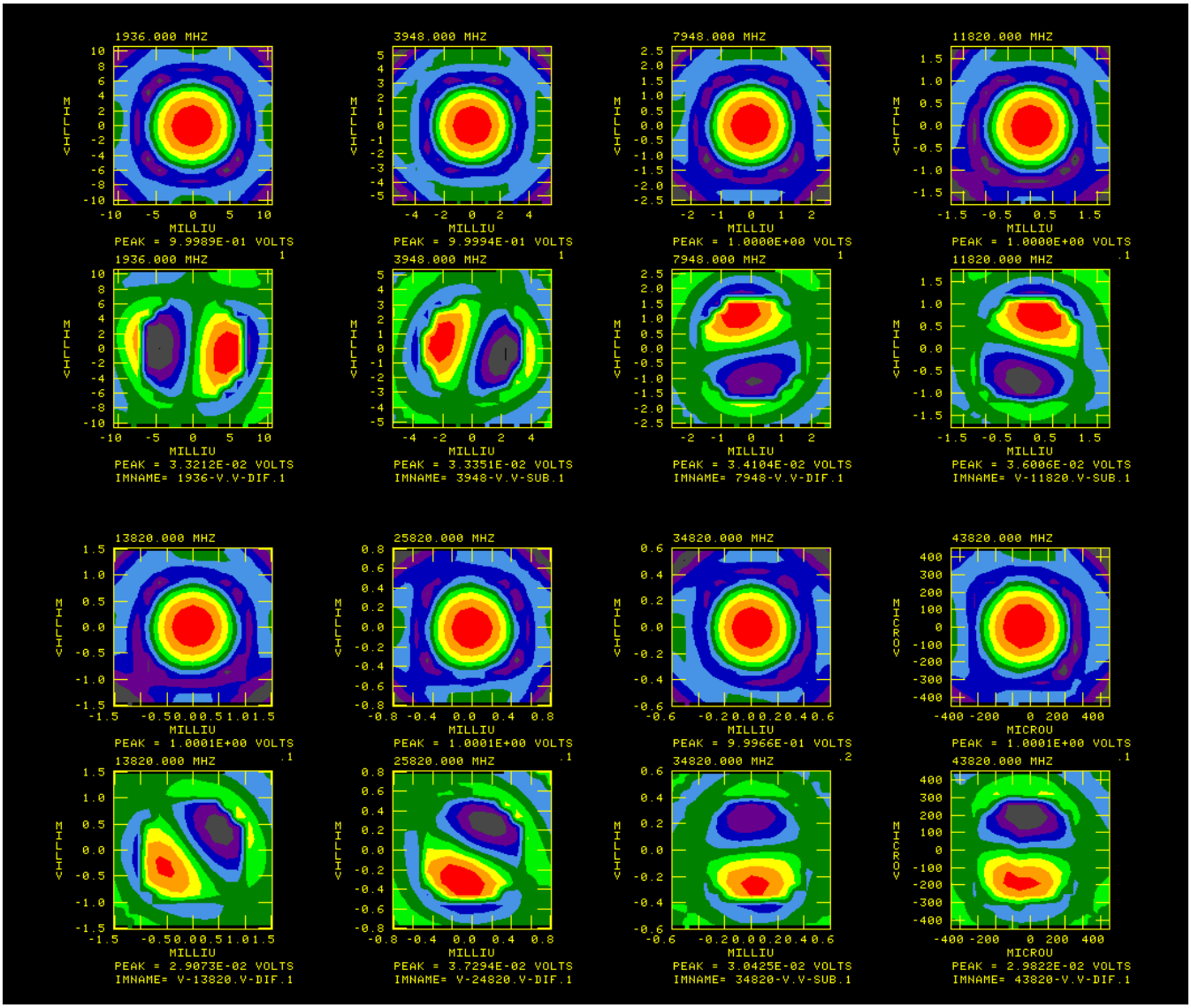

Figure 23: (I,V) voltage beam pairs for the eight cassegrain bands, with I above and V below. All images are normalized to unity power in 'I'. The frequency increases from right to left and from top to bottom, so L-band (1936 MHz) is in the upper left, and Q-band (43820 MHz) in the bottom right. The color coding for the 'I' beams utilizes a logarithmic transfer function, with the transition from blue to green corresponding to 4% power (-14 dB), and the transition from light to dark blue at 1.4% power (-18 dB). The 'V' images utilize a linear transfer function, from −3.5% to +3.5%. Dark green spans zero, transitioning to blue at −10%, and to light green at +10% of the peak voltage. The line separating the signed responses is oriented with the position of the feed.

This is either a calibration issue, or one arising from a lack of understanding – but it has not yet been investigated, due to other pressing priorities.

6.3 Acknowledgments

This work could not have been done without the significant assistance of Ken Sowinski, Michiel Brentjens and Bryan Butler, who were instrumental in development of the holography beam scanning programs, and Eric Greisen, who modified and expanded the holography calibration and imaging programs 'UVHOL' and 'HOLOG', and the beam measurement program 'PBEAM'. Thanks also to Ken Sowinski, Eric Griesen, and Emmanuel Momjian for finding significant typographical errors in an earlier version.

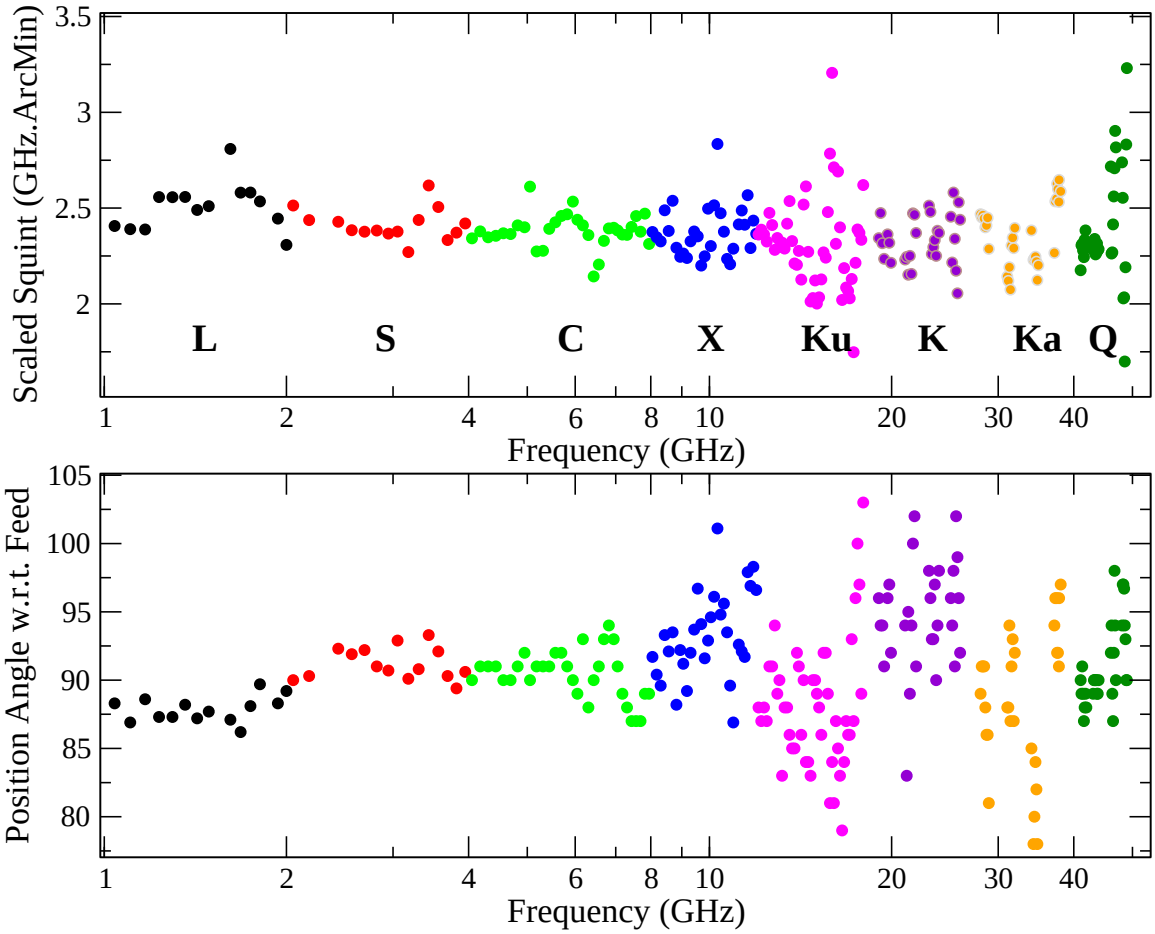

Figure 24: The squint separation and position angle for all spectral windows. (Top) The normalized angular separation between the RCP and LCP beams – divide by the frequency in GHz to derive the physical separation. (Bottom) The position angle on the sky of the line joining the peaks in the RCP and LCP beams with respect to the position angle of the feed w.r.t. the center of the primary reflector.